

## Effective methods for removing different types of dyes – modelling analysis, statistical physics treatment and DFT calculations: a review

M.G. El-Desouky<sup>a,\*</sup>, M.A.G. Khalil<sup>b</sup>, M.A.M. El-Affify<sup>a</sup>, A.A. El-Bindary<sup>c</sup>,  
M.A. El-Bindary<sup>d</sup>

<sup>a</sup>Egyptian Propylene and Polypropylene Company, Port Said 42526, Egypt, email: ch.moh.gamal@gmail.com (M.G. El-Desouky)  
ORCID ID: <https://orcid.org/0000-0001-6060-463X>

<sup>b</sup>Chemistry Department, Faculty of Science, Port Said University, Port Said 42511, Egypt, emails: magomaa@hotmail.com (M.A.G. Khalil)  
ORCID Id: <https://orcid.org/0000-0003-0653-2289>, maher.elafffy@yahoo.com (M.A.M. El-Affify) ORCID Id: <https://orcid.org/0000-0002-8764-7303>

<sup>c</sup>Chemistry Department, Faculty of Science, Damietta University, Damietta 34517, Egypt, email: abindary@yahoo.com (A.A. El-Bindary)  
ORCID Id: <https://orcid.org/0000-0002-4494-3436>

<sup>d</sup>Basic Science Department, Higher Institute of Engineering and Technology, New Damietta, Egypt,  
email: m.a\_bindary@yahoo.com (M.A. El-Bindary) ORCID Id: <https://orcid.org/0000-0001-5977-1465>

Received 23 July 2022; Accepted 11 October 2022

---

### ABSTRACT

Organic dyes, a class of highly poisonous and carcinogenic chemicals that pose serious health risks to humans and aquatic life, are the most prevalent organic pollutants found in wastewater from sectors such as textiles, rubber, and cosmetics. Organic dyes, a class of highly poisonous and carcinogenic chemicals that pose serious health risks to humans and aquatic life, are the most prevalent organic pollutants found in wastewater from sectors such as textiles, rubber, and cosmetics. This review compares and contrasts several dye removal processes. Adsorption has proved to be a quick and efficient way to get colours out of wastewater. This research focuses on the most recent developments in porous materials for organic dye adsorption. Dyes were used to color food and other industrial items, textiles, plastics, cosmetics, and tannery. Non-ionic dyes, cationic dyes (basic dyes), and acid dyes are the three types of dyes (dispersed dyes). The process of removing dyes from sewage from industry has become increasingly essential from an environmental standpoint. In an aqueous system, cationic dyes have a net positive charge due to their sulphonate groups, while anionic dyes have a net negative charge. To avoid contamination of the aquatic environment, these waste dyes must be handled first. This dye's aromatic composition offers it increased durability and makes it tough to decompose. Color wastes were removed from waste water via oxidation, electrochemistry, coagulation, solvent extraction, photocatalytic degradation, ozonation, and adsorption, among other ways. However, the adsorption process is more advantageous than other ways. As a result of its ease of use, high effectiveness, simple design, easy availability of adsorbents, and most importantly, its low cost. Different porous materials' properties, functionalization, and modification are also discussed. Also discussed are the adsorption behaviors and mechanisms of these adsorbents in the adsorption of organic dyes. Finally, future research challenges and opportunities in the development of innovative materials for very efficient dye removal are suggested.

*Keywords:* Dyes; Adsorbents; Photocatalytic degradation

---

\* Corresponding author.

## 1. Introduction

Dye production is one of the businesses that contributes the most chemicals to sewage. Textile factories are producing more than 700,000 tons of dyes that are among the top three contaminants. Most reactive colorants are toxic and have a risk of teratogenic and carcinogenic mutations [1]. The origin of the dyes was much later, when the indigo blue dye was found in mummy wrappings in Egyptian tombs 4,000 y ago, it revolutionized the dye industry. An organic colourant was discovered for the first time [2]. Around the world, there are more than 100,000 commercially available dyes, and 7,107 tons of colourants are produced year [3–5].

Water is a crucial component of the Earth's environment is a necessary element of life. As the population and living standards rise, so does the need for water, which is rising daily [6,7]. Our water resources' quality is declining daily as a result of the persistent introduction of harmful substances into them. The residues of medicines and other drugs (new emerging pollutants) in water are among the most dangerous contaminants [8]. These contaminants are extremely hazardous because they can interfere with human enzymatic, hormonal, and genetic systems [9]. Therefore, it is necessary and important to get rid of these chemical and pharmaceutical residues in water before to provide the neighborhood with water. According to the 2004 French Plan of National Sant Environment (PNSE), it is required to check these pollutants in water before supplying it to the population. In a nutshell, a growing topic of research is the elimination of these new developing contaminants and contemporary necessity in environmental science. Therefore, academics, researchers, doctors, and regulatory agencies are concerned with getting drugs and pharmaceuticals out of water [10].

The technique that seems to be the most useful and effective is adsorption. It allows for the almost complete removal of hazardous contaminants at low concentrations [11]. The kind of adsorption material employed affects how well different contaminants are removed. One of the categories for these materials suggests that they can be divided into natural and synthetic ones [12]. The first category consists of carbons of diverse natural origins, chalk and clay rocks, ash, peat, slag, zeolites, vermiculites, and sand [13]. The second-category of adsorbents consists of silica gels made from variously treated mineral raw materials, synthetic zeolites, titanium and zirconium hydroxides or phosphates, activated carbons, ion exchange resins, and polymers with chelate groups. The current situation of anthropogenic aquatic media is problematic, and the majority of the available adsorption materials are unable to sufficiently remove dangerous pollutants from wastewater. As a result, it is essential to use advanced technologies that have much large specific surface areas and that have also been modified with different chemically active groups to improve adsorption activity and selectivity. Research efforts at many scientific schools are focused on creating materials whose adsorption capacity is several times more than that of traditional adsorbents such activated carbon, zeolites, clays, etc. as a result of the rapid expansion of the nanotechnology industry [14].

The fashion factories today use mostly direct dyes, for example, synthetic organic dyes, dyes for manufacturing, reactive dyes, and so on. Wide range of colorants and chemicals used to make common shades of fabrics more appealing to competitive market render them very complex. Environmental concerns associated with the production and application of colorants have evolved dramatically over the past decade and are undoubtedly among the main driving forces affecting the textile dye industry today. The term "natural dyes" is used to describe any dye that comes from an organic source, such as plants, animals, or minerals. Natural colours are generally insufficiently pigmented and must be added to textiles using mordents, they are often metal salts that have a preference for the colouring agent as well as the fiber. Numerous businesses, notably the garment industry, frequently use synthetic dyes.

As early as 1856, Perkin was the pioneer in the development of manmade organic dye, mauve. The first organic synthetic dye was developed at 1871, as Woulfe treated the natural dye, indigo with nitric acid, to prepare picric acid [15,16]. The fashion industries account for nearly 70% of the highest use of dyestuffs. Disperse dye are the largest market with a share of about 21% followed by direct dyes and reactive dyes of 16% and 11%, respectively. Textile dyes are usually graded either according based on their chemically makeup or their application.

Many adsorbents have been created and modified in recent years to be used in the adsorption of organic dyes. Despite several excellent evaluations that compile numerous related papers, the category of adsorbents in each review is highly different and contentious because there is no universally accepted criterion for adsorbents for dye removal. The purpose of this work is to present recent developments, with a particular emphasis on innovative porous materials for the adsorption of dyes from a wide angle. The technologies used to remove dyes and their negative consequences are outlined in this review. This work offers fresh perspectives on the creation of innovative porous materials, in particular with regard to their properties and use in the adsorption of dyes. A straightforward classification system was also suggested for the choice of typical adsorbents. Additionally, this review identifies the crucial elements affecting the adsorption mechanism [17]. This paper also emphasizes adsorption isotherm, adsorption kinetics, and adsorption mechanism. Although several materials exhibit excellent adsorption abilities, many of them have not yet been developed for use on an industrial scale and have their own limits. Based on these facts, a thorough examination of the problems, the knowledge gap, and the outlook for the future is presented at the end. In the future, we hope that this work will serve as motivation for the development and use of new adsorbents. Dyes very in resistance to sunlight, suddenness washing, air, alkalis, and other chemicals; in their sensitivity to specific fibers; their solubility and application process, as well as their reactivity to cleaning chemicals and methods [18].

## 2. Classification of dyes

Table 1 summarizes the classifications of dyes based on their use, this is organized in accordance with the

classification of the applications. For every application class, it displays the main substrates, application techniques, and typical chemical kinds. However not depicted in Table 1, dyes are also utilized in high-tech fields such as medicine, electronics, and non-impact printing. For instance, they are utilized in ink-jet printing, direct and thermal transfer printing, photocopying (photocopying and laser printing), and electrophotography (both toner and organic photoconductor). As in customary uses, azo dyes predominate; other colours utilized include phthalocyanine, anthraquinone, xanthene, and triphenylmethane. The volume of these applications is currently modest (between tens of kilos and several hundred tons annually) high added value, though (a few hundred to several thousand dollars per kg), having rapid growth rates (up to 60%).

### 2.1. Acid dyes

Such colors, in pH range 3.0–7.0, can be applied to cotton, wool or silk. Such dyes wet-fastness ranges from moderate to excellent and their luminosity is usually 5.0–6.0 in the blue-scale range. Acidified solutions (formic or acetic acid) are commonly used to synthesize the dyes, with the degree of acidity varying depending on the dye's qualities. Acid dyes are usually vivid and may be washed at various speeds. The dye molecules differ widely in composition and contain complex metals.

The group's distinguishing characteristic is the existence of sulphonated unit, which give water-solubility. Bonding

to wool occurs partly on the wool fiber due to contact with these groups of sulphonated and groups of ammonium (Figs. S1 and S2). The Van der Waals forces have extra bonding interactions (Tables S1 and S2). Anionic dyes are chromophoric azo systems (the most important group), anthraquinone, triphenylmethane or copper phthalocyanine, which are soluble in water by addition of one to four classes of sulphonates Tables S3 and S4. The example of these dyes is shown in Fig. 1.

### 2.2. Basic dyes

Most commonly used to colour acrylic fibers, basic dyes are water soluble. The majority of the time, they are observed with a mordant (Figs. S3 and S4). A reagent is a chemical substance that helps to set colours on textiles by forming an insoluble compound with the dye.

Basic colouring, aside from acrylic, is not particularly good for any other fiber because it is difficult to light Tables 5 and 8, wash, or rapidly change colours (Fig. 2). They are thus typically used to offer fabrics that have already been colored with acid colored with acid colors after treatment (Tables S5–S7).

### 2.3. Azo dyes

Dyes classified as chromophores the presence of an azo group ( $-N=N-$ ). Are used in numerous types of industrial dye, make up about one-half of all synthesized dyes and mostly used in the clothing, fruit, paper, printing, leather

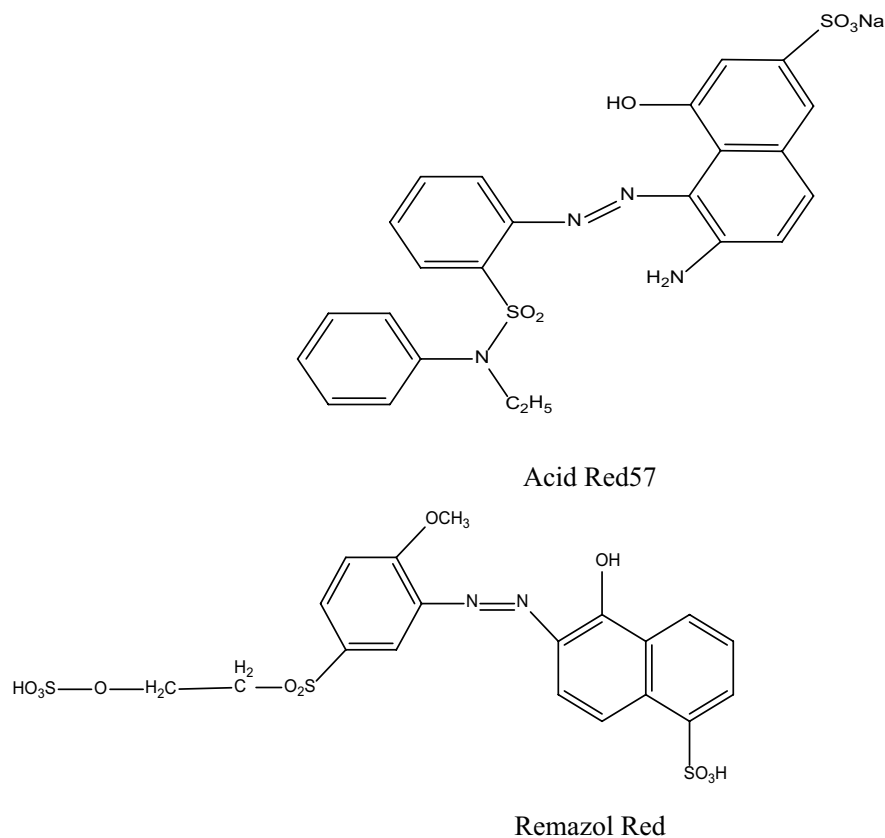


Fig. 1. Examples of acid dyes.

and synthetic cosmetics. Azo colors are structurally diverse, However, the existence of an azo linkage, that is,  $N=N$ , is their most notable structural trait. Because this bond can happen many times, monoazo dyes only possess one azo relation, whereas diazo dyes have two and triazo dyes have three. Sulphonated azo dyes are azo dyes that contain substituent sulfonate groups [19,20]. Azo groups create a complex structure that enables dyes to display a wide

spectrum of colours when paired with aromatic substituents or enolizable groups (Fig. 3).

#### 2.4. Reactive dyes

Reactive dyes create a chemical compound when they interact with fiber molecules. These dyes are made from alkaline solutions or neutral solutions that are then alkalinized in a different phase. Heat treatment is occasionally used to get different hues. [21]. To avoid unfixed dye, the fabric is cleaned thoroughly with soap after tinting. Originally, only active dyes were employed on cellulose fibers, but they are currently used in various (Fig. 4).

#### 2.5. Vat dyes

Vat colouring is insoluble in water and cannot stain textiles directly. We can be made soluble, however, by lowering the alkaline solution that allows textile fibers to be attached. Dye is returned to its insoluble state by after that, there is oxidation or sun exposure. Original vat dye is indigo. Those colors, including cotton, linen and rayon are the best colors [22,23]. They are used to dye other fabrics like wool, nylon, polyesters, acrylics and modacrylics with mordants. Fig. 5 describes the usual chemical structures of vat dyes.

#### 2.6. Sulphur dyes

Using caustic soda and sodium sulfide, sulfur colorant are insoluble and can be designed to be soluble. Dyeing is achieved with huge amounts of salt at high temperature, in order for the colour to permeate the fabric [24]. Extra colorants and additives completely washed away. These colors

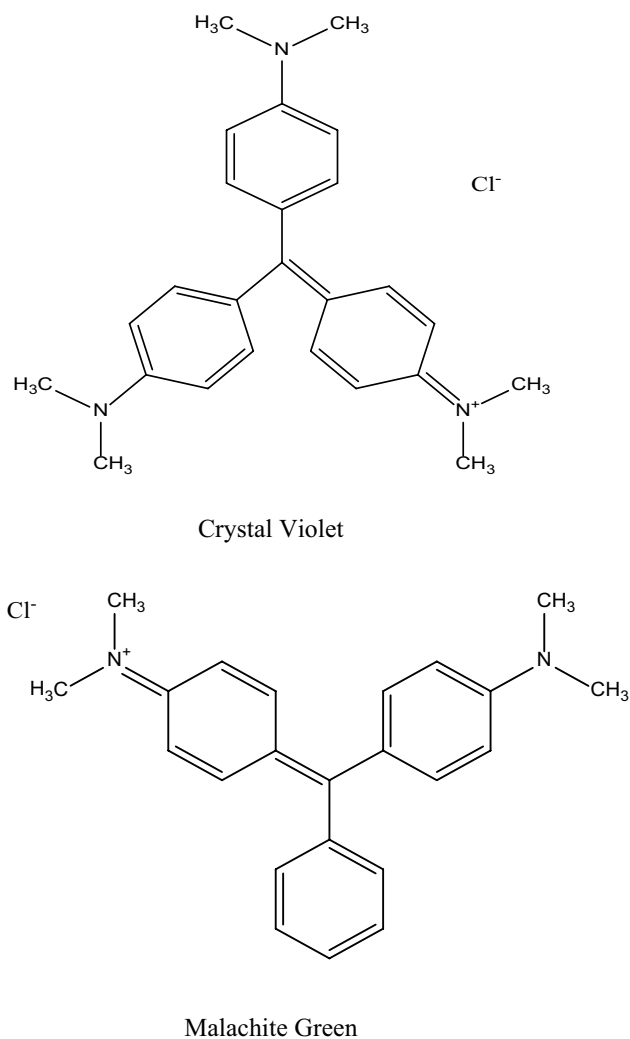


Fig. 2. Example of basic dyes.

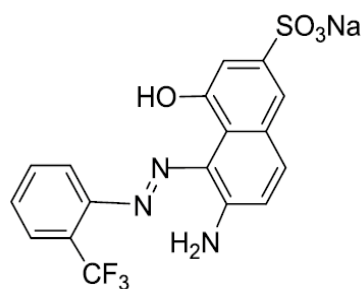


Fig. 3. Example azo dye.

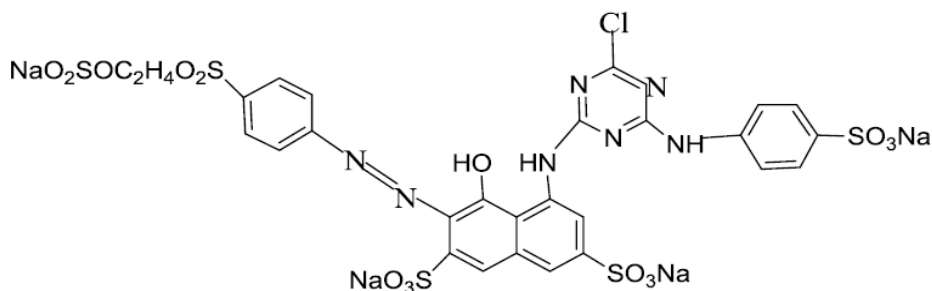


Fig. 4. Dye (C.I. Reactive Red 198).

are easy to light, to wash and to suddenly use mostly for cotton and linen (Fig. 6).

### 2.7. Disperse dyes

Insoluble in water characteristic for dispersed colorant. Such colors are finely ground can be utilized in the form of a paste or powder that dissolves in water. These substances breakdown and colour the fibers [25,26]. Initially created for cellulose acetate coloring, these dyes are already commonly used to color nylon, cellulose triacetate, and acrylic

fibers as well. A typical disperse dye structure is shown in Fig. 7.

### 2.8. Direct dyes

Without using mordents, direct colors effectively stain cellulose fibres. We've colored wool, silk, nylon, cotton, rayon, and a variety of other materials [27,28]. As they're very simple to light, such colors are not extremely bright and have a slow washing time. The basic dye is given as an example in Fig. 8.

Table 1  
Usage and classification of dyes

Class	Principal substrates	Description	Method of application	Chemical types
Acid	Leather, paper, inks, wool, silk, and nylon	Anionic chemicals that are water-soluble	Usually from neutral to acidic dyebaths	Azo (including pre-metallized), anthraquinone, triphenylmethane, azine, xanthene, nitro and nitroso
Basic	Paper, polyacrylonitrile, modified nylon, polyester and inks	Water-soluble, applied in weakly acidic dyebaths; very bright dyes	Applied from acidic dyebaths	Cyanine, hemicyanine, diazahemicyanine, diphenylmethane, triarylmethane, azo, azine, xanthene, acridine, oxazine, and anthraquinone
Direct	Cotton, rayon, paper, leather and nylon	Water-soluble, anionic compounds; can be applied directly to cellulose without mordants (or metals like chromium and copper)	Applied from neutral or slightly alkaline baths containing additional electrolyte	Azo, phthalocyanine, stilbene, and oxazine
Disperse	Polyester, polyamide, acetate, acrylic and plastics	Not water-soluble	Fine aqueous dispersions often applied by high temperature/pressure or lower temperature carrier methods; dye may be padded on cloth and baked on or thermofield	Azo, anthraquinone, styryl, nitro, and benzodifuranone
Reactive	Cotton, wool, silk, and nylon	Water-soluble, anionic compounds; largest dye class	Reactive site on dye reacts with functional group on fiber to bind dye covalently under influence of heat and pH (alkaline)	Azo, anthraquinone, phthalocyanine, formazan, oxazine, and basic
Sulfur	Cotton and rayon	Organic compounds containing sulfur or sodium sulfide	Aromatic substrate vatted with sodium sulfide and reoxidized to insoluble sulfur-containing products on fiber	Indeterminate structures
Vat	Cotton, rayon, and wool	Oldest dyes; more chemically complex; water-insoluble	Water-insoluble dyes solubilized by reducing with sodium hydrogen sulfite, then exhausted on fiber and reoxidized	Anthraquinone (including polycyclic quinones) and indigoids

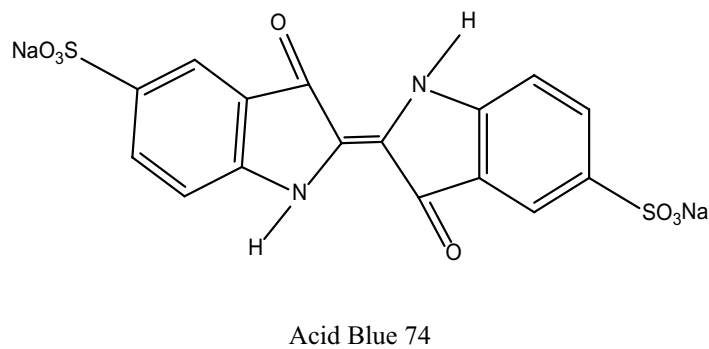
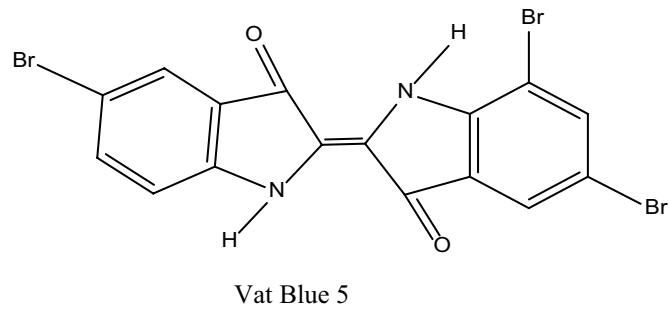
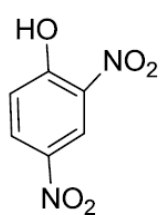
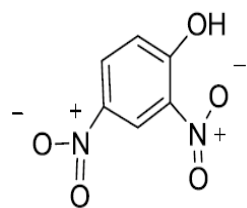


Fig. 5. Chemical structure of vat dyes.



Leuco Sulfur Black 1



Sulfur black

Fig. 6. Two sulfur dyes were use.

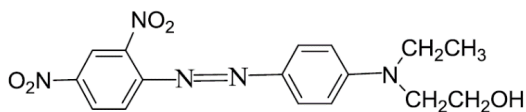


Fig. 7. Chemical structure of C.I. Disperse Red 8.

### 2.9. Classification of dyes by use or application method

### 3. Toxicology and toxicity assessments

Over 30 years ago, the Western European Industry that produces colourants started looking into the toxicological and ecological effects of dyes, long before chemical and environmental restrictions existed (and pigments). Currently, a slew of laws and regulations mandate that manufacturers examine the hazard potential of each of their products.

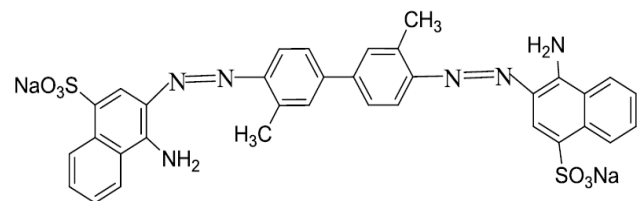


Fig. 8. Direct red 2.

Toxicology research focuses on a multitude of topics, the most important of which is with (1) acute toxicity, (2) irritation of skin and eyes, (3) toxicity after repeated application, (4) sensitization, (5) mutagenicity, and (6) cancerogenicity.

#### 3.1. Acute toxicity

The first step in evaluating whether dyes are harmful is to properly evaluate or assess their acute toxicity, as defined by the EU Directive 67/548/EEC (with numerous amendments). A detailed analysis of such data, including skin and eye irritation, was collected from safety data sheets for a number of commercial dyes, demonstrated that the risk of these acute toxic consequences (also known as “harmful” or “toxic”) was extremely low. Although the review is from a long time ago, the conclusions can be assumed to be still true today [29].

#### 3.2. Sensitization

Textile dyes are suspected to be the source of skin responses, according to dermatologists. Some reactive dyes can cause contact dermatitis, allergic conjunctivitis, rhinitis,

occupational asthma, and other allergic reactions in textile workers. The propensity of reactive dyes to mix with human serum albumin is thought to be the cause (HSA) to give a dye–HSA conjugate which acts as an antigen. The antigen then creates particular immunoglobulin E (IgE) antibodies, which cause allergic reactions via the production of intermediates such as histamine [30]. A study of 414 workers who had dye powder exposure, in 1985, a survey of workers in the dye industry, including those in mixers, weighers, dyehouse operators, and laboratories. Twenty-one of them were found to have allergic reactions to one or more reactive colours, including occupational asthma. ETAD published a list of reactive dyes that induced respiratory or cutaneous sensitization in workers exposed to them on the job. These colours should be labelled appropriately in the EU, as they are all classified in the European Inventory of Existing Chemical Substances (EINECS).

Utilizing liquid dyes will help you prevent exposure to colour dust, to lessen the risk, use personal protective equipment and colours with low-dusting formulations. Reactive dyes have various toxicological properties since the reactive group is no longer present after dyeing and fixing, additionally, the wearer's flesh won't be exposed due to the high fastness qualities. As a result, no allergic reactions have been documented in people who have worn reactive coloured textiles.

Textile contact is thought to be responsible for 1%–2% of all allergy disorders treated in German hospitals, with dyes accounting for the majority of them. Disperse dyes were the most noticeable, especially when used for skin-tight, close-fitting clothing composed of synthetic fabrics. Sweat fastness qualities of dyes on various textiles play a big role in whether or not an allergic reaction is triggered. If coloured on polyamide or semi-acetate, where the low wet fastness allows the dyes to move to the skin, sensitizing disperse dyes may produce allergic skin reactions. In the 1980s, several severe allergic reactions were linked to polyamide stockings and pantyhose's, and in the 1990s, sportswear (leggings) made of semi-acetate.

There has been no legal prohibition in any country to date, but some organizations, such as the International Association for Research and Testing in the Field of Textile Ecology (ko-Tex), which awards eco-labels to environmentally and toxicologically proven textiles, refuse to award eco-labels to certain dyes [31].

### 3.3. Mutagenicity

Some dyes are mutagenic in nature. The Ames test is a common initial screening procedure for evaluating a chemical's mutagenicity. It is a process for creating bacterial point mutation tests that uses specific bacterial strains *Salmonella typhimurium* with histidine-dependent growth.

A point mutation is identified by a dose-dependent reversion to histidine-independent growth. It was discovered that the Prival test, an adaptation of the Ames test, was superior for mutagenicity testing of azo dyes. This test imitates how an animal's reductive enzymatic cleavage of the azobond breaks it down [31].

It is commonly accepted that the development of cancer is a multiphase process, with the initiating phase being

particularly susceptible to the effects of genotoxic agents. The bacterial reverse mutation test is a very sensitive assay for the development of point mutations in bacteria rather than a test for the complex multiple step process of carcinogenesis in mammals, hence a strong relationship between Ames test results and mouse cancer bioassays cannot be envisaged. Validation tests reveal a weak correlation between the endpoints of mutagenicity in bacteria and carcinogenicity in rats.

A chromosomal aberration assay should be performed if these findings indicate a possibility for mutagenicity, a potential next step would be a cytogenetic test in vitro. After proving a genotoxic potential in vitro, equivalent in vivo investigations must be carried out in order to determine a possibly mutagenic potential in animals. After proving a genotoxic potential in vitro, equivalent in vivo investigations must be carried out in order to determine a possibly mutagenic potential in animals. The test results may also enable the estimation of a substance's carcinogenic potential [32].

### 3.4. Carcinogenicity

Some dyes and intermediates have been known to be harmful for quite some time. The effects of acute, or short-term, exposure are well understood. They're kept in check by maintaining chemical concentrations in the workplace under strict guidelines and preventing physical contact with the material. Chronic effects, on the other hand, are often not noticeable for many years after exposure. Higher rates of benign and malignant tumours, particularly in the bladders of employees exposed to various intermediate and dye manufacturing procedures, according to statistics, during the years 1930–1960, dye-producing countries recorded an increase in production. The chemicals in question were 2-naphthylamine [91-59-8,4-aminobiphenyl [92-67-1], benzidine (4,4-diaminobiphenyl) [92-87-5], fuchsine (C.I. Basic Violet 14, 42510 [632-99-5]), and auramine (C.I. Solvent Yellow 2, 11020 [60-11-7]). There's a lot of evidence that these substances' metabolites are the ones that cause cancer. In most industrialised countries, strict rules governing the handling of recognised carcinogens have been enacted Table 2. Almost all dye businesses have stopped using these chemicals as a result of the rules. Some colours have been proved carcinogens in animal experiments and are likely carcinogens in humans [33,34].

## 4. Methods of dye removal

Dye techniques of elimination involve just initial water treatment techniques like equalization and sediment are carried out. Since there was no dye discharge cap for effluent.

Following the establishment of appropriate coloring effluent release requirements, highly effective decolorization processes, including colouring filter beds and the activated sludge process, were implemented. Thereafter a color sewage treatment plant shown in Fig. 9 was the first of its kind. Technique, referred to as the conventional colorant elimination processes, used by the manufacturing concerned a while before discontinued because of the high price operating and preservation. Many works are currently under

Table 2  
Different chemicals used in textile chemicals processing

Type	Example
Acid	Acetic acid, formic acid
Alkali	Sodium hydroxide, potassium hydroxide, sodium carbonate
Blach	Hydrogen peroxide, sodium hypochlorite, sodium chlorite
Dyes	Reactive, direct, disperse, pigment, vat
Salt	Sodium chlorite
Size	Starch, PVA
Stabilizer	Sodium silicate, sodium nitrate, organic stabilizers
Surfactant	Detergent
Auxiliary finishes	Fire retardant, softner

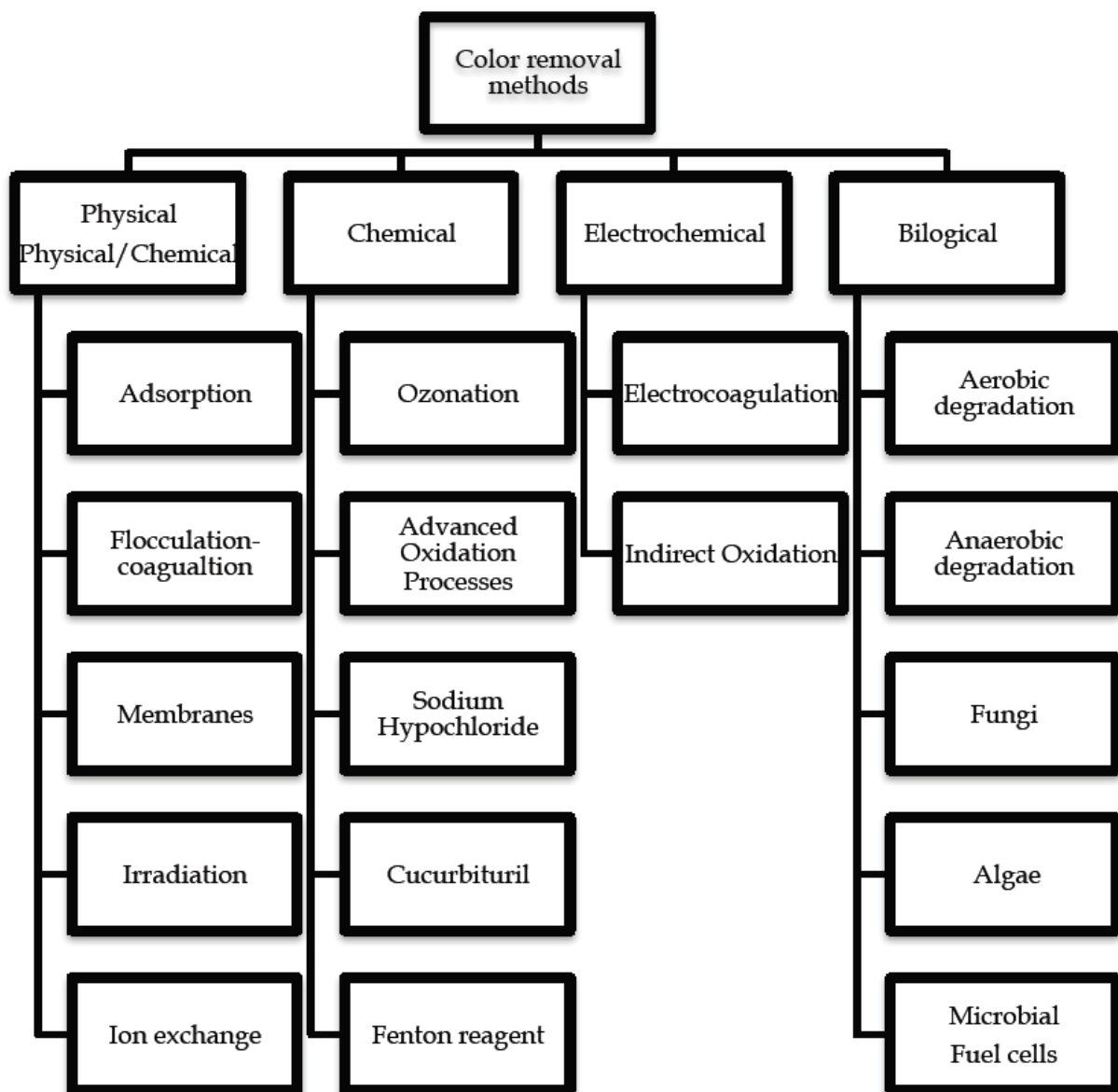


Fig. 9. Techniques for removing colour from textile effluent.

way to find the best form of extracting dye as a result of which dye discharge can be captured and recycled [35–39].

#### 4.1. Biological dye removal approaches

The standard biological approach for treating dye waste water is the widely and extensively used color removal processes in most countries. A mixture of aerobic and anaerobic processes is commonly regarded as the traditional procedure, prior to the discharge of colored effluents into the atmosphere process has been colorants method of choice processes primarily since it is relatively low-cost and straightforward to complete. Furthermore, this procedure is inadequate to entirely remove dangerous materials of textile wastewater, hence why coloured water can still be found in the atmosphere.

While traditional approach reduce need for in waste water, there is a chemical oxygen present. Certain traditional methods for extracting biological dye biomass of microbe's adsorption, algal decomposition, enzyme decomposition, fungus farms, microbiological cultures, and pure or mixed plants are all examples of deterioration. Aforementioned processes in Table 3 laterally their definition, benefits and disadvantages. Methods for extracting biological dye integrate some type of living organism into their operation. This approach should be used with caution, and it should be maintained in engineering ethics.

#### 4.2. Chemical procedures for removing dye

Chemical dye extraction procedures are those that employ chemical or its principles to remove the color. Accelerated oxidation, electrochemical destruction, elimination of the Fenton reaction dye, oxidation, zonation, photochemical, and ultraviolet irradiation are all traditional ways for removing chemical dye. Numerous chemical removal efficiency techniques are more costly than biological and physical dye removal techniques, with the exception of electrochemical degradation removal efficiency technologies. Chemical colour removal methods are frequently unappealing to businesses, necessitate specialized equipment, and use a lot of electricity [40].

The strength of apparatus or units that remove chemical colors necessitates a lot of electricity. Furthermore, large-scale chemical and reagent usage is a well-documented issue among chemical decolorization technique users [40]. Other undesirable aspect of these methods is the development of

harmful secondary contamination that occurs after chemical dye removal, posing a new disposal difficulty.

#### 4.3. Physical techniques of dye removal

Methods of physical sorption process is usually a simple procedure. Generally employed by the processes of mass transportation adsorption, coagulation or flocculation, ion exchange, and other conventional procedures for removing visible dye are used. Radiation, filtration of membranes, nanofiltration, or ultrafiltration and reverse osmosis.

Such approaches commonly selected their easiness and effectiveness. Biological and chemical decolorization techniques pale in comparison, process needs by far the least amounts of chemicals [41]. This approach is considered more dependable than the other two dye extraction procedures because it does not involve living creatures.

#### 4.4. Electrochemical methods

In the mid 1990's electrocoagulation techniques were developed. Efficient means to extracting ink. This technique utilizes make the relationship among metal electrodes in the effluent, including aluminium and iron, to enable the metal plates move to dissolve in waste water.

$\text{Fe}(\text{OH})_3$ , dissolved dyes may be extracted by precipitation or flotation. This approach demonstrates high productivity with respect to color removal and recalcitrant pollutants degradation [42–44].

### 5. Efficiency of dye elimination techniques

Various approaches of treating effluents from holding dye. Despite the fact that there are several methods available. Only a few examples include coagulation, chemical oxidation, membrane filtration, electrochemistry, and aerobic and anaerobic microbial decomposition Tables 3–5.

#### 5.1. Sedimentation

Primary method of most municipal wastewater treatment facilities use this technique plants [45]. Variety processes alternatives to choose from for improving suspended particle gravity settlement, chemical flocculants, sedimentation basins, and clarifiers are only a few examples Fig. 10.

Table 3  
Advantages and disadvantages of chemical treatments

Methods	Advantages	Disadvantages
Treatments with chemicals		
Process of oxidation	Technology that is easier to use	( $\text{H}_2\text{O}$ ) The agent must be activated in some way
(Reagent of Fenton)	Fenton's reagent is an excellent chemical tool	Generating sediment
Ozonation	Ozone must be utilized in its gaseous condition because it does not increase the volume of wastewater or sediment	Half-life short (20 min)
Photochemical	There is no sediment formed, and bad odors are much decreased	By-product's creation
NaOCl	Begins and increases azo-bond cleavage	Unleashes of aromatic amines

Table 4  
Physical and electrochemical treatments have advantages and downsides

Methods	Advantages	Disadvantages
Treatments that are physical		
Activated carbon adsorption	Effective treatment different colorant	Extremely costly
Filtration using membranes	All types of dye are eliminated	Generated heavy sediment
Exchange of ions	There is no loss of adsorbent during regeneration	Not all dyes were successful
Irradiation	Efficient laboratory oxidation	Need much O <sub>2</sub> dissolved
Electro kinetic coagulation	Economically workable	Strong development of sludge
Electrochemical treatments		
Destruction through electrochemistry	There are no chemicals used, and there is no sludge build-up	Flow rates that are unusually high are a strong indicator

Table 5  
Benefits and drawbacks of biological therapy

Methods	Advantages	Disadvantages
Biological treatments		
White-rot fungus cause discoloration	Colorants can be degraded by white-rot fungi via enzymes	The generation of enzymes has also shown to be unreliable
Microbes from other cultures (mixed bacterial)	Decolored in 24–30 h	Under aerobic conditions, azo hues are not easily digested
Living/dead microbial biomass adsorption	Some colorants have a strong affinity for microbial organisms	All dyes were unsuccessful
Textile-dye bioremediation systems that are anaerobic	Under water-soluble dyes, azo must be decolored	Methane and hydrogen sulphide are produced during anaerobic decomposition

### 5.2. Filtration technology

An integral component application for Microfiltration, ultrafiltration, nanofiltration, and reverse osmosis are used to purify drinking water and remediate wastewater. This was investigated for deleting the color [45]. For a specific water treatment purpose, each membrane method has its own set of advantages and disadvantages. Among them, microfiltration is of little use in because of its wide pores, it is suitable for wastewater treatment, and while ultrafiltration and nanofiltration are two types of filtrations techniques successful in dye molecules clog membrane pores frequently, making separation techniques for textile wastewater treatment ineffective Fig. 10.

### 5.3. Chemical treatment

A coagulating/flocculating agent is used to treat dye chemically from waste water is one of the effective ways to extract pigment [46,47]. The cycle includes introducing agents' effluent, for example (Al<sup>3+</sup>), (Ca<sup>2+</sup>) or (Fe<sup>3+</sup>) ions, and produces flocculation's. In addition to these other agents were also used for the operation combination of two can also be applied often to enhance the process Fig. 11.

### 5.4. Oxidation

Oxidation is a system using oxidizing agents to waste water. Two methods usually *viz.* For treating effluents, particularly those obtained from initial treatment, chemical oxidation and UV assisted oxidation with chlorine, hydrogen peroxide, Fenton's reagent, ozone, or potassium permanganate are utilized (sedimentation). Because they require small amounts and quick reaction periods, they are among the most extensively utilized procedures for discoloration processes. They are used to break down dyes partially or entirely. On the other hand, full oxidation of the dye theoretically breaks down complex molecules into carbon dioxide and water. The importance of pH and catalysts in the oxidation process should not be underestimated.

### 5.5. Electrochemical methodology

The removal of color is often used as a tertiary therapy. Decoloration can be accomplished either via consumable ingredients or electrocoagulation. Several types of anodes are available, such as titanium, conducting. The electro-degradation of dyes has been effectively carried out using boron doped diamond electrodes and other experimental conditions [48].

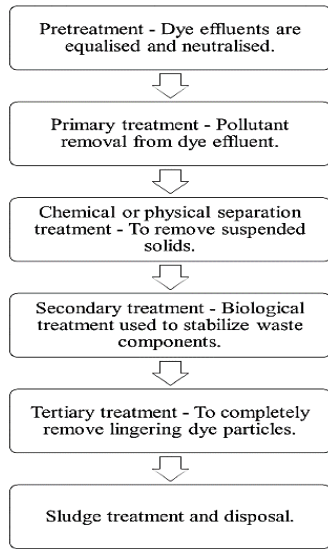


Fig. 10. Traditional wastewater treatment system.

5.6. Advanced oxidation processes (AOPs)

System requiring using multiple oxidation processes at the same time, because a single oxidation system is frequently insufficient for full colour degradation. Advanced oxidation processes (AOPs) are reactions that include the rapid formation of the highly reactive hydroxyl free radical, such as Fenton’s reagent oxidation, UV photolysis, and sonolysis. They can breakdown colours at room temperature and pressure, and they may be a better option than biological treatment for waste streams containing hazardous or bio-inhibitory contaminants [49].

5.6.1. Photocatalysis

It also one of several efficient contaminant breakdown and oxidation methods [49,50]. A catalyst’s valence band electron is excited into the conduction band by light energy from a light source, resulting in the creation of hydroxyl radicals through a series of reactions. Because hydroxyl radicals have a strong oxidation proclivity, they can attack and oxidize almost any organic structure.

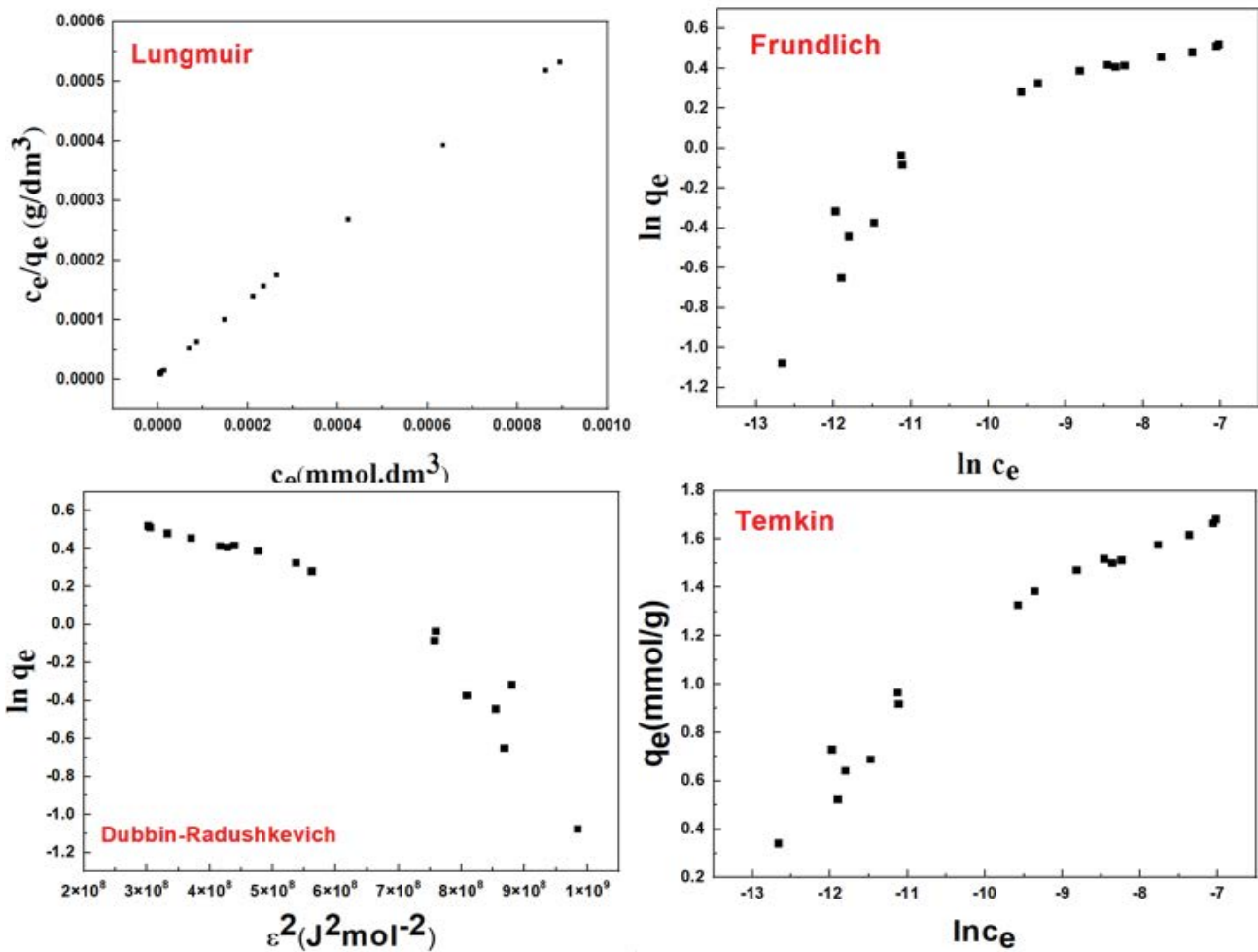


Fig. 11. Linearized plots of adsorption isotherm models of MB at ZIF-8.

### 5.6.2. Sonolysis

Application of ultrasonic waves was used to decolorize and degrade colorant. Proposed a generic process for sonochemical reactions focused on the emergence of transient species during strong cavitation episodes [51].

### 5.7. Biological treatment

This is the most successful and commonly used method for treating dyeing waste water [51–53]. A large number of organisms were used to decolorize and mineralize different dyes. The technique provides many advantages, such as being comparatively cheap, small operation charges and not being harmful to the end products of full mine realization.

### 5.8. Aerobic treatment

The most investigated microorganisms for their ability to remediate coloured wastewaters are bacteria and fungus. When in an aerobic setting, the organic compounds are broken down by enzymes secreted by bacteria found in wastewater. The task at hand to classify and isolate microorganisms that are aerobic that can degrade numerous colorants that ongoing for in excess of two decades [53].

### 5.9. Fungal strains

Fungal strains various have studied in depth the strains of fungi that can decoloring azo and triple phenyl methane colorants. *Phanerochaete chrysosporium*, has thoroughly It has being researched for its capacity to decolorize a widespread variety of colors by numerous works over the past two decades [54,55]. In addition to this microorganisms such as *Rhizopus oryzae*, *Cyathus bulleri*, *Coriolus versicolor*, *Funalia trogii*, *Laetiporus sulphureus*, *Streptomyces* sp., *Trametes versicolor* and other microorganisms have also been checked for decolorization of colorants. Specific parameters, as an example pollutants dose of pollutants, dyestuff concentration, temperature and initial pH, influence the procedure of decolorization.

### 5.10. Anaerobic treatment

Ability methods for anaerobic digestion for the decomposition of a wide range of materials of synthetic dyes has been well-proven and confirmed. While some recent attempts to decolorate although dyes have performed well in aerobic environments, the prevalent belief that almost all azo dyes are non-biodegradable persists in the conventional aerobic energy system [56].

### 5.11. Treatment that is both aerobic and anaerobic

A treatment that includes both aerobic and anaerobic components is suggested to provide promising results for the purpose of obtain improved cleaning of colored complexes derived by textile industries. A benefit such a method, mineralization in total that frequently completed thanks to the mutually beneficial behavior a variety of

organisms. In addition, the azo bond has the capability of reduction can accomplished below reduced environments in anerobic bioreactors and resulting aromatic amines that are colourless and odourless can. The combination anaerobic-azo dye treatment method is appealing since it mineralizes under aerobic circumstances [57–60].

### 5.12. Ion exchange

Ion exchange is a chemical process that can be reversed in which an ion from a solution is exchanged for an ion that is equally charged but bound to a stationary solid particle [61]. Change of ions together with adsorption for industrial and fixed-bed purposes, these techniques can be classed together as “sorption processes” for unified treatment of high-quality water. Ion exchange has also proved successful in the elimination of colours.

### 5.13. Adsorption

Adsorption is a method that can be used to treat industrial wastewater in addition to having a wide range of applications. In addition to being commonly used for removal of dyes. The term adsorption refers to phase where a substance is extracted out of its liquid or gaseous environment absorbed at a solid surface. The adsorption method is considered In addition to initial effectiveness, it outperforms alternative reclaimed water technologies, design simple, ease of use, and inconsideration to toxic substances [62].

Adsorption is considered a flexible technology for water and waste water treatment since adsorbent can also be used to achieve very high rates of contaminant removal [63,64]. Adsorption was widely used in the separation and purification of industrial products. The removal of colorful and colorless organic species from industrial waste water is seen as a significant application of adsorption processes. Adsorption method is used for removal.

The basic characteristic of an adsorption processes material collection on the surface. Differentiating between two forms of adsorption is now a customary. If, in fact, attractiveness exists between both the solid surface and the attached particles, the adsorption is called direct adsorption (physisorption) [65].

In most cases, Van der Waals forces present the attractive forces is physical adsorption between both the particles that have been adsorbed and the solid surface, they are naturally weak, allowing in reversible adsorption. Treatment systems are referred to as chemisorption when the interaction energy is resistant to chemical bonding. Despite the stronger bonding in chemisorption, removing adsorbed species from a solid surface is difficult. Variables including dye content, starting pH, and discharge temperature can all affect the decolorization procedure. While this strategy is cost-effective, and biological treatments are excellent for a wide spectrum of colours, the main disadvantages of biological treatments include the colours' poor biodegradability.

In terms of style and operation, there will be less flexibility greater aquatic requirements and longer time needed for the operation of color removal, rendering impossible to extract effluent dyes in liquid fermentation on a continuous basis.

The use of adsorbents will also remove any colours that are hard to break down biologically. An excellent adsorbent [66] must have a high porosity (resulted in a wide surface area) as well as the time it takes to reach adsorption equilibrium is as low as feasible so that it may be used to remove color waste quickly. Adsorbent had the advantage of being reusable, as it can be used more than three times.

## 6. Adsorbents mainly used for dye waste water treatment

### 6.1. Alumina

Alumina a porosity crystalline gel that is manufactured and affordable in various size particles with a range of surface areas 200–300 m<sup>2</sup>/g [67].

### 6.2. Silica gel

Coagulated with the creation of porosity and abrasive surfaces is caused by colloidal silicic acid, non-crystalline granules of varying thickness. This exhibits a comparison to alumina, it has a larger surface areas, ranging from 250 to 900 m<sup>2</sup>/g [67].

### 6.3. Zeolites

Zeolites are significant naturally occurring as well as synthetically manufactured microporous adsorbents. They also go by the name “selective adsorbents,” which highlights the importance of ion exchange and molecular adsorption [68–70].

### 6.4. Activated carbon

Activated carbon is the first adsorbent that has been discovered, and it is typically made from coal, coconut shells, lignite, wood, and other materials using one of two methods: chemical vs. physical [71–73].

### 6.5. Glycidyl methacrylate magnetite

Polymers have some major advantages over other adsorbent materials; for instance, polymers could easily manufactured in a variety of situations physicochemical properties (scale, scale distribution, porosity, hydrophobicity, etc.) and can be changed by inserting different ligands into the structure to create unique sorbents. Macroporous crosslinked glycidyl methacrylate (GMA) copolymers, developed by radical suspension copolymerization, in the form of standards beads of required size and porosity, have already been used successfully for heavy and precious metal sorption as well as for dye adsorbents.

Epoxy groups have one special ability to react. They undergo ring opening with specific compounds that have groupings of hydroxyl, amine, or activated methylene. Of this reason, in mild reaction conditions, polymers with epoxy (oxirane) groups give various functionalizing possibilities. Oxirane-functioning polymers are rare.

Examples of these polymer are epoxidized polybutadiene and phenol-formaldehyde resins with glycidyl groups [74]. Glycidyl methacrylate is the only vinyl monomer currently available to hold group oxirane.

### 6.6. Nanosphere magnetic metal oxide

Specific metal oxide for example, Fe<sub>3</sub>O<sub>4</sub>, Fe<sub>2</sub>O<sub>3</sub>, MnO, Al<sub>2</sub>O<sub>3</sub>, TiO<sub>2</sub>, MgO, ZnO and Ce<sub>2</sub>O<sub>3</sub> nanoparticles have been utilized as an adsorbent pollutant removal [75]. Among them, iron-based material has been attracted by several researchers because of long-term stability, biocompatibility, amphoteric surface efficiency, enhanced functional role, and dispensability are all factors to consider ( $\alpha$ -Fe<sub>2</sub>O<sub>3</sub>) is the under the much more sustainable iron oxide atmospheric environments that is broadly catalysts, pigments, sensors, gas filtration, and water recycling are just a few of the applications also porous magnetite nanoparticles (Fe<sub>3</sub>O<sub>4</sub>), have received a great agreement of consideration due to their appealing applications especially like a fascinating family of crystal structures [76]. Nano-scaled magnetite has been considerable interest concerning to the size and shape-controlled synthesis recent magnetic separation now is common among used in the fields of medicine, diagnostics, molecular biology, bioinorganic chemistry and catalysis. Magnetic separation can be one of the promising ways for a novel technique of environmental purification due to the potential to generate no pollutants such as flocculants and to processes large amounts of wastewater in a short time. However, this approach is specially adapted when the separation problem is complex, that is, when contaminated water includes solid residues that exclude their treatment in column with regards to the risks of filling. Magnetic systems often used in environmental applications are industrial carriers consisting of magnetite particles distributed in a cross-linked polymer matrix [77]. The removal of clothing effluent dyes is of great importance [78]. The release of colors into the atmosphere reflects only a small proportion of water contamination, but due to their brightness, coloring is evident in limited amounts. At the other hand, their presence inside industrial effluents also influences the processes of photosynthesis. Therefore, a low-cost method needs to be identified that is efficient in extracting dyes from large amounts of effluents (Table 6).

### 6.7. Metal–organic frameworks (MOFs)

Metal–organic frameworks (MOFs) are porous crystalline materials they're very well their numerous applications that are well known for their various application (Table 7). MOF materials are of particular interest due to the simple tuning of their pore size and their high surface area. MOFs also commonly used in plant of gasses and adsorption, isolation, and storing of vapors [90].

### 6.8. Nanomaterials made of polymers

The drawback of nanoparticle agglomeration or sintered, that diminishes the surface area of these nanoparticles and decreases their contact areas [99], along with superior tensile characteristics, easy handling, high degree of dispersion, and relatively inexpensive [100,101], Use of polymers in waste water treatment has attracted a lot of attention. Such nanoparticles were routinely synthesized in polymers for consistent distribution of nanoparticles and enhanced conductivity of the polymeric nanocomposite

while processing industrial effluents. Polyaniline, polypyrrole, polyparaphenylene vinylene, polyparaphenylene, polythiophene, polyacetylene, and others are components of additional savings with higher tensile strength across all sorts of photodegradation due to its exceptional reliability, easy fabrication, and quality in transporting high range that can be functionalized (by HCl, H<sub>2</sub>SO<sub>4</sub> etc.). Şen et al. [102] to investigate the impact of pH, temperature, and the initial quantity of methylene blue on the reaction kinetics of adsorption between both the composite and the color, researchers utilised a composite film made of polyethylene (GCP) and green clay (MB) [102]. According to the findings, increasing the MB content boosts adsorption, boosting the pH from 5.5 to 9. The kinetic energy of the molecules increases, leading to a rise in temperature. In addition, the pseudo-second-order model was the most accurate kinetic and thermodynamic model of adsorption. ( $\Delta G$ : 70.64 kJ/mol,  $\Delta S$ : 70.64 J/mol·K,  $E_a$ : 12.37 kJ/mol at 308°C) revealed that adsorption was spontaneous, physical, and low-energy

[103]. Gouthaman et al. [103] polyaniline-polyvinylpyrrolidone (PAPV) and polyaniline-polyvinylpyrrolidone neodymium/ZnO (PAPV-NZO) polymeric nanocomposites were effectively synthesized and characterized by oxidation polymerization and used as adsorbents in the discharge of Acid red 52 colour with various parameters including time and adsorbent dosage. Due to the combination of NZO, which increases the conductivity, stability, and surface area of PAPV-NZO with the requisite dye concentration and adsorbent dose of PAPV-NZO, PAPV-NZO has a larger dye removal rate than PAPV ppm and 50 mg, respectively. Moreover, in good conditions (pH 14 2, 0.05 g of adsorbent dosage with 3% N NZO in 80 ppm dye), PAPV-NZO was removed 99.6% using the Langmuir model, pseudo-second-order kinetics, with the  $q_{max}$  of PAPV-NZO estimated to be 159.36 mg/g. Mohammadikish and Jahanshiri [104]. Two metal-based interaction polymers were produced (Pb<sup>2+</sup>-FSL, Zn<sup>2+</sup>-FSL) to assist in the degradation of dissolved colors (methylene blue (MB), methyl orange

Table 6

Absorption coefficient comparisons ( $q_m$ ) of porous magnetic nanosphere iron oxide and various adsorbents for both RB5 and CR dye

Adsorbents	Maximum adsorption capacity (mg/g)		References
	CR	RB5	
Dolomite	72.4	229.2	[79]
Banana peel powder	49.2	164.6	[80]
MgO FA	48.8	–	[81]
Use of <i>Macrocystis pyrifera</i> biomass and zero-valent iron nanoparticles	39.9	–	[82]
Fe <sub>3</sub> O <sub>4</sub>	18.0	–	[83]
MoO <sub>2</sub> /CaSO <sub>4</sub> composites		853.3	[84]
Hierarchical C/NiO-ZnO composite	–	613	[85]
Hydroxyapatite nanoparticles loaded on Zn	–	416.7	[81]
Amine-modified Biomass of <i>Funalia trogii</i>	–	193.7	[86]
Pineapple plant steam	–	12.0	[87]
PEI-CW	77.5	34.4	[88]
Porous magnetic nanosphere iron oxide	1,070	1,621.59	[89]

Table 7

Absorption coefficient comparing ( $q_m$ ) of zeolitic imidazolate framework-8 and various adsorbents for both Malachite green dye

Adsorbent	$q_m$ (mg/g)	References
Using coconut fiber, activated carbon was created from coconut coir	27.44	[91]
SWCNT-COOH	19.84	[92]
Iron humate	19.2	[93]
Nanowires of Cd(OH) <sub>2</sub> placed on activated carbon	19	[94]
MWCNT-COOH	11.73	[95]
SWCNTs	4.928	[94]
SWCNT-NH <sub>2</sub>	6.134	[94]
Activated carbons commercial grade (ACC)	8.27	[92]
Bentonite clay	7.716	[96]
Activated charcoal	0.179	[97]
ZIF-8	60.27	[98]

(MO)) The elimination of cationic MB was excellent for both coordination polymers when the dye adsorption performance of the synthesised coordination polymers was investigated (97.2% for Pb coordination polymer and 99.9% for due to the larger negative surface charge of Zn<sup>2+</sup>-FSL, the elimination efficiency of anionic methyl orange in the case of Pb coordination polymer is significantly greater (97.2%) in comparison to the situation of Zn coordination polymer (23.1%). Furthermore, the pseudo-second-order kinetics model was used to fit the adsorption kinetics of both MB and MO onto Pb<sup>2+</sup>-FSL and Zn<sup>2+</sup>-FSL [104,105].

### 6.9. Carbonaceous nanomaterials

Carbon nanotubes (CNTs) are hollow cylindrical graphite micro-crystals with excellent mechanical qualities long-term stability, unusual electrical characteristics, and large specific surface areas are just a few of the benefits.

Such nanoparticles have large surface areas and amorphous microporous surfaces, and they're used in industries to remove adsorbent dose, particularly once one liquid element in a combination has to be preferentially adsorbed [106].

Despite the fact that CNTs get a high dye adsorption rate capability owing of its hollowed and multilayer nanostructured nanostructures architectures, they possess big particular regions and are expensive prevents them from being used in industry.

Furthermore, because to their tiny size, strong aggregation, and curing capabilities, CNTs hard to remove from water-based solutions. Considering expense issue and CNT extraction via water environments can be overcome [107] as a sustainable matrix for CNTs, by building CNT composites using polymers, carbon, metal oxide, and other materials. CNTs have lately been exploited as a potential nano-filler in CNT-based nanocomposite with excellent adsorption, electrical, mechanical, and thermal properties, making CNT-based composites efficient adsorbents. It is not just adds to the number of active places, but also expands the area covered. Areas vs. their primary materials CNTs/ACF composites, CNTs/Fe<sub>3</sub>O<sub>4</sub> composites, CNTs/dolomite composites, CNTs/cellulose composites, and CNTs/graphene composites are examples of these composites. Also, by reducing aggregate formation the adsorption capabilities of CNTs can be improved by making them more hydrophilic in character, that results in the highest selectivity for the adsorption of ionic species from aqueous media due to the presence of oxygen-containing groups at the surface [108].

Dawood et al. [109] purified CNTs manufactured by catalytic chemical vapour deposition (CCVD) process and utilised as an adsorbent to eliminate dyes (BO) and (MV). Different effects of parameter were studied. The greatest clearance of methyl violet and basic orange dyes was achieved at pH 14.85 and CNT dosages of 0.25 and 0.3 g/L, respectively [110].

The percentage of dye adsorption was shown to be per the Kumar et al. [110], dyes are much are inversely proportional, although contact time is directly related.

The equilibrium reactive black (RB) adsorption is strongly aligned to the Langmuir and Temkin isotherms, and the pseudo-second-order model better represented adsorption kinetics. As per Dutta et al. [111], MWCNT and

ACNT had a better affinity for cationic MG, MB, and RhB dyes, while NH<sub>2</sub>CNT had a binds to receptors for anionic dye MO [111].

The Langmuir equilibrium isotherm model also fitted MG adsorption by ACNT, HCNT, MWCNT, and MO adsorption by NH<sub>2</sub>CNT, with adsorption capacities of 198.41 (MWCNT), 194.55 (ACNT), 167.78 (HCNT), and 194.55 (NH<sub>2</sub>CNT) mg/g, respectively. The usage of the sorbents was also assessed, and it was discovered that after three consecutive runs, they retained their efficiency (96%).

### 6.10. Nanofibers

Nanofiber is a polymer fiber with a diameter ranging from 1 to 1,000 nm. A nanofiber absorbent has It has a surface areas and length-to-diameter ratio, indicating that it has a lot of surface area and a lot of adsorption active sites. Separation requires only a minimal number of nanofibers, resulting in a considerable decrease in desorption solvent volume [112]. CNFs have evolved as an important choice considering the low cost and ease of manufacture of tiny tunable pore sizes in comparison to other adsorbents owing to the increase expense of utilizing adsorbents like CNTs and graphene in industrial topics. Techniques for producing nanofibers include spinning of melt, solution, emulsion, and electro, with electro spinning being most common.

In principle, vapor-grown CNFs (VGCNFs) and electro spun CNFs (ECNFs) are the two types of CNFs based on their production, with the ECNFs being used in water purification [113].

When compared to VGCNFs, electro spun nanofibers have higher pore densities, they are much more effective as water and air filtration because they have a greater surface area per unit volume, lower and upper secondary pollutants, higher permeability, a lower base weight, and a smaller fiber diameter. When compared to cast polymer membranes, electro spun nanofibers have the drawback of being mechanically unstable. Unless a nanofiber will have all the listed functions, it helps to consider a function. This is usually achieved by placing other materials or arranging special surface structures, which helps improve the capabilities of embedded composites or structured nanofibers with a large surface area and is one of the reasons why nanofibers have become popular in recent years. Ibupoto et al. [114] found that activated carbon nanofibers had a remarkable adsorption efficiency, completely decolorizing the dye solution within 60 min of contact time, with adsorption data following the Langmuir isotherm model with a  $q_{max}$  of 72.46 mg/g and best suited to the pseudo-second-order kinetic model [114].

In Cheng et al. [115], DA@PDA nanofibers were used to remove MB out of an aqueous phase inquiries. After 30 h of interaction, the DA@PDA nanofiber was shown to have an adsorption strength of approximately to 88.2 mg/g at a temperature of 25°C and a pH of 6.5 [116].

Because of the electrostatic attraction between the surface functional groups of the O-EC, it was found that porous carbon nanofibers had a remarkable absorption capacity, completely conditions or disables the dye solution within 60 min of contact hours, of adsorption data going to follow the Langmuir isotherm model with a  $q_{max}$  of 72.46 mg/g and best suited to the pseudo-second-order kinetic model, with

adsorption data following the Langmuir isotherm mode [117]. At 25°C, electrospinning carbon nanofibers (ECNFs) functionalized with MB dye had a greater affinity (170 mg/g) than virgin ECNFs (32.5 mg/g). Thermodynamic research ( $\Delta G$ : 11.089 kJ/mol at 298 K;  $\Delta H$ : 89.975 kJ/mol) revealed that MB adsorption onto O-ECNFs was endothermic and spontaneous [117].

### 6.11. Xerogels and aerogels

Xerogels and aerogels are desirable possibilities as adsorbents and catalyst support materials for a variety of applications due to their huge surface areas, low cost, high porosity, internal pore volume, and low density [117].

To make xerogels and aerogels with an appropriate porous structure, excellent mechanical characteristics, and distinct granule microstructures, the sol–gel process is being used. These highly adsorbent particles are also chemically and thermally stable, have a high sorption capacity even after regeneration, and have a significant reactivity toward a variety of substances, includes pollution gases and metal ions. According to Wu et al. [118], xerogels have a number of advantages, having the ability to make them in specified shapes or thin films, easy extraction from sample solution, and control over physical properties including hydrophobicity, porosity, and optical properties. Xerogels come in three different forms: crystalline, amorphous, and g-forms (silica gel) (alumina). Aerogels have more surface area, porosity, and pore volume than xerogels, as evidenced by alumina aerogels, that have a high surface area of 1,000 m<sup>2</sup>/g and a pore volume of 17.3 cm<sup>3</sup>/g while retaining all other xerogel characteristics. However, there is a scarcity of information about their adsorption properties. Wu et al. wanted to know how factors like solution pH, textural properties, hydrophobicity, and hydrogen bonding affect adsorption efficiency [118]. The adsorption of four organic dyes (methyl orange, alizarin red S, brilliant blue FCF, and phenol red) on porous xerogels made to use a two-step sol–gel technique was examined. With increasing solution pH, electrostatic repulsion between the dyes and the xerogel surface reduced adsorption, whereas the combined effects of increased hydrophobicity or pore size/volume of the xerogels enhanced adsorption capacity [119].

Kaya et al. [120] employed volcanic tuff to make silica xerogel, which they then used as an adsorbent to remove methylene blue (MB). Temperature had the greatest effect, accounting for 54.50% of the variance in beginning MB concentrations, contact time, silica xerogel dose, temperature, and pH are all variables that can be controlled. MB percentage removal of 96.18% and optimum adsorption ability of 51.967 mg/g were reached under optimum conditions of 60 min contact time, initial MB concentration of 20 ppm, silica xerogel dose of 0.0016 g/L, temperature of 40°C, and pH 5. The maximum desorption accuracy was 88%, with the silica xerogel retaining around 70% of adsorption efficiency after five cycles [120].

Han et al. [121] two types of silica aerogels as adsorbents to remove distinct dyes: one hydrophilic (hydroxyl-group) and one hydrophobic (surface modified) (MSA) (HSA). The goal was to see how these colours adsorb to different aerogel characteristics. After four regeneration cycles, the MSA

aerogel including a high surface area of 880.47 m<sup>2</sup>/g used to have an adsorption capability of 65.74 mg/g for MB and 134.25 mg/g for RhB, as well as an adsorption effectiveness of around 90%. The HSA aerogel with a specific surface area of 628.52 m<sup>2</sup>/g had a  $q_{\max}$  of 47.21 mg/g for MB and 185.61 mg/g for RhB after the third reuse cycle, as well as an adsorption accuracy of over 80% [121].

## 7. Biosorption

### 7.1. Biosorption fundamental

Biosorption (biotechnological method) is an applied part of environmental sustainability) [122]. It is regarded as an environmentally benign, cost-effective, and efficient water treatment method. It keeps the concentrations of various contaminants in the water within the permitted limits set by various federal rules [123]. This green approach is in line with green chemistry concepts. The principles of the biosorption process, as well as its various constituents, must be understood. In a nutshell, it is a procedure that is not dependent on metabolism (passive uptake) according to the use of biological effluent as well as removal various pollutants in the water. In general, the recycling of these biomasses results in a slew of advantages. Use they have natural forms that have been altered contributes straight to trash reduction [124].

This the ability to solve a wide range of ecological and environmental issues. It also has notable characteristics such as minimal operating and manufacturing costs, as well as great efficiency.

### 7.2. Biosorption strategy

Biosorption has been evolving in recent years as a multidimensionally successful method. When compared to other traditional wastewater treatment methods, it is regarded as an excellent alternative. Sorption is a physicochemical process when sorbate molecules connect to another substance's surface (sorber). Effluents that have been purified of excellent quality are produced as a result of this. Despite the use of the “bio” prefix to indicate a biological entity's involvement, the term “biosorption” has a simple definition. In terms of the sorption mechanism, both bio-absorption and biosorption dimensions play a role. The transfer of a material from one state to another is known as absorption. It comprises gas absorption by aqueous solution or liquid absorption by a solid). Adsorption is a chemical bond, but it's also a physical one between a sorber and a sorbate that results in a sorber-sorbate interface, adsorption is a chemical bond [125]. In a nutshell, biosorption is a passive, physiologically unaffected process that encompasses all aspects of sorbate-biomatrix interaction (biosorbent). It is important in a variety of processes that occur spontaneously in several scientific fields [126].

### 7.3. Biosorbents selectivity

Appropriate biosorbent choice is thought to become the most important factor to consider when choosing one. The price of biomass and where it comes from are important factors to consider when choosing a biosorbent. To be used

for the manufacture of various biosorbents, dead biomass takes precedence over live biomass [127]. There are numerous benefits to using dead biomass. It can be summarized as follows: (1) No need to include growing demands (such as media and minerals) in the bulk solution; (2) There are no toxicity restrictions; (3) Reuse and recoveries of saturating biosorption and adsorb contaminants are both conceivable; and (4) Modeling of contaminant absorption that is more mathematically and statistically simple. Furthermore, the biosorbent chosen must meet a number of criteria, including environmental friendliness, Biocompatibility, availability, and feasibility are all factors that must be considered. This ensures its ability to detoxify a variety of contaminants found in water. Biosorbent must also possess a variety of other appealing characteristics. This is demonstrated by its strong high sorption effectiveness vs. contaminants, exceptional durability, and renewability. Recyclability and adaptation of the biosorbent to varied designs (e.g., batch, fixed bed systems) should be taken into account [128]. Based on the concept of trash as wealth, the available wastes should be given priority. Because of their environmental friendliness, they can be used for a variety of purposes. It's cost-effective because it solves disposal issues while also generating cash for a variety of sectors. The abundant organic materials, in truth, are structurally quite different [129].

Amongst ligands that make it up these molecules are alcohol, amino, aldehydes, carboxylic, hydroxyl, phosphate, thiol, ketones, phenolic, and ether groups. They can interact with target pollutants through a variety of processes since they are present in variable degrees.

Biosorption is a promising approach that can be used instead of traditional methods. It is contingent on with use of bio-waste to remove many types of contaminants from water. Its premise is based on the idea of getting two uses out of bio-waste. This is accomplished by recycling material in order to directly contribute to waste reduction while also maximising the advantages obtained [130].

As a result, it is possible to meet the emission reduction targets set by international or national rules, as well as the World Health Organization (WHO) [131]. It stands out for its reduced operational and product attribute, as well as flexibility, ease of use, and effectiveness, are all advantages chitosan (ii) biochar [132]; (iii) activated carbon [133]; (iv) bio-nanocomposites; (v) bio-hydrogels [134]; (vi) Alternative and effective sorbents based on marine algae are being studied for wastewater treatment. It takes into account globally distributed renewable resources. Color and colloid content are used to classify it. *Chlorophyta*, *Phaeophyta*, and *Rhodophyta* algae are the three basic kinds of algae found in oceans. Recent research has established the usage of microalgae as a viable option.

For instance, Afshariani and Roosta [135] investigated methylene blue sorption in aqueous solutions using batch and continuous methods. The greatest sorption was 87.69 mg/g at a pH of 9 and a temperature of 30°C. As an additional leather coloring absorbent, puree microalgae biomass (microalgae biofuel effluent) was explored. Aqueous dye solutions of Acid blue 161 were used to conduct biosorption tests (AB-161). At 25°C and 40°C, respectively, 75.78 and 83.2 mg/g of dye were adsorbed, respectively. Biomass reduced dye amount by 76.65% in effluents from

a real tannery, according to the data. Alginate, carrageenan, and polycolloid make comprise the cell wall of algae, is primarily made up of polysaccharides. These elements are capable of the removal of a wide range of pollutants from water [136]. Both macro and microalgae have been used as ideal options to produce various organic dyes, in addition to the removal of toxic metals from aquatic systems [137].

A green macroalga (*Enteromorpha flexuosa*) was tested for its ability both crystal violet (CV) and methylene blue (MB) were extracted from aqueous solutions. Under optimal settings of parameters for CV and MB, percentage elimination of 90.3% and 93.4%, respectively, were obtained [138].

Green algae are mostly made up of cellulose, which is mixed with polysaccharides to make glycoproteins. There are numerous functional groups (as amino, hydroxyl, and carboxyl) describe these molecules. They are extremely important in the sorption process [139,140].

Fucoidans, mannitol, laminarins, fucoxanthin, halogenated compounds, polyphenols, and terpenoids are all examples of alginates are some of the metabolites that distinguish brown algae [141]. Salts of calcium, phosphate, and sodium used to make alginates. The brown seaweed cell wall is primarily composed of sodium salts. Its weight has increased by about 30%–40%. Polysaccharides that are anionic, linear, and water soluble. Brown seaweed alginate was obtained using a variety of pre-extraction preparation procedures [141]. These natural biopolymers are widely used in a variety of applications in the environment.

It is frequently employed as a possible sorbent for removing different pollutants from water [142]. It refers to possessing diverse functional groups.

Several researchers examined biochar generated heavy metals elimination from aqueous solution using microalgae pyrolysis as another type of sorbent. A batch system has been used to test biochar for Co(II) elimination efficiency Freundlich, Temkin, and D–R isotherms all well-fitting by equilibrium data. 1.117 mg/g was the Langmuir biosorption capability [143]. Water dracaenas are used to make biochar (*Eichhornia crassipes*) has been shown a good sorbent material for removing heavy metals and a way to control this invasive plant. Using water hyacinth biomass as a biochar feedstock has a number of advantages. The added benefit of decreasing the species' impact on delicate aquatic ecosystems as an invasive species. The maximal sorption capacities of biochar-alginate capsules for the value of extracting cadmium from an aqueous solution varied from 24.2 to 45.8 mg/g [144]. At 55°C, the greatest biosorption ability for ytterbium was 0.642 mmol/g, according to the equilibrium research. Calcium carbonate was utilized to manufacture sodium alginate-based beads with various concentrations of pore-forming agent to improve the sorption capabilities of alginate gel beads [145]. Cu(II) adsorption capacity raised by at minimum a factor of two (from 13.69 to 33.88 mg/g) according to the experimental results [145]. Other experimental technique for alginate was to phosphorylate alginate-PEI beads and use them for the sorption of Nd(III) and Mo(VI) [146]. Phosphorylation increases the sorption of Nd(III) significantly, but phosphorus groups have a more restricted effect on Mo(VI). Nd(III) maximal capacity to absorb increased from 0.61 to 1.46 mmol/g after phosphorylation of alginate-PEI beads.

Because molybdate species have a high affinity for amine groups [146], the increase in Mo(VI) absorption substantially decreased pronounced (from 1.46 to 2.09 mmol/g) [147].

Chitosan is a type of chitin that has been modified. It's mostly fashioned from either crab or shrimp shells [128]. The sorption qualities of six distinct crosslinking agents used to crosslink chitosan sorbents were compared three ionic agents: sodium citrate, sodium tripolyphosphate, and sulfosuccinic acid, as well as three covalent agents: glutaraldehyde, epichlorohydrin, trimethylolpropane, and triglycidyl ether [148]. The chitosan hydrogel's reactivity to the Reactive Black 5 dye was dramatically influenced by ionic crosslinking [148]. After 24 h of sorption, chitosan cross-linked with sodium citrate and sulfosuccinate had a sorption potential of 46.7% and 37.2%, respectively, as compared to non-crosslinked chitosan [148]. Chitosan had been bonded with glutaraldehyde and trimethylolpropane triglycidyl ether after 24 h of sorption. 35.3% and 26.6% lower sorption potentials than unmodified chitosan, respectively. The unmodified chitosan had the highest sorption capacity (2,307 mg/g), the absorbent capabilities of the ionically crosslinked hydrogels ranged from 2,005 to 2,164 mg/g. The adsorption capabilities of the covalently chemically bonded hydrogels were 2,083–2,183 mg/g [148]. To eliminate (CV) and (MO) from wastewater, a polypyrrole-decorated chitosan-based mag-sorbent was created. At the ideal conditions, CV and MO removal performance was 88.11 and 92.89%, respectively.

The dynamics of pseudo-second-order accurately approximated CV removal, whereas the PSO closely matched MO's. The Langmuir adsorption isotherm for CV and MO was quite near to the estimates of adsorption equilibrium, with maximal potentials of sorption in monolayers of 62.89 and 89.29 mg/g, respectively. Immobilization of chitosan on another polymer is another means of modifying it. Chitosan, for illustration, was finally converted using 4-methyl-2-(naphthalen-2-yl)-N-propylpentanamide functionalized ethoxy-silica and then tested for MB and AB 25 [149]. Adsorption produce of MB was 3 times higher with composite beads compared with chitosan beads, and 1.4 times higher with AB 25. Other chitosan hybrid composite with a saturated adsorption capacity of 627 mg/g was created by doping a small amount of chitosan and Y(III) ions onto acid-modified fly ash (named MFA) [150]. The researchers worked hard to improve chitosan's selectivity for certain metal ions. Chitosan microparticles grafted with 2-mercaptobenzimidazole, for example, extremely sorbents that are selective to be developed. Magnetite particles are also a key component in making chitosan microparticles easier to use and recover. The sorbent was shown to have a high selectivity for precious metals as compared to base metals. Elwakeel et al. [151] found that combining chitosan with 2-MBI results in a highly efficient sorbent for recovering valuable metals from acidic leachates. Batch experiments were used to evaluate heavy metal ions (Mn, Fe, Co, Ni, Cu and Zn) have different adsorption capacities on chitosan than their comparable anions,  $\text{SO}_4$ ,  $\text{Cl}^-$ , and  $\text{NO}_3$ . Using column tests, the selectivity of a number of heavy metal ions was evaluated. Both the sulphate ions and the heavy metal cations in the sulphate salts, adsorb to a far greater amount than the comparable  $\text{Cl}^-$ , and  $\text{NO}_3$  salts. [152].

Luo et al. [153] developed a luminous to effectively eliminate Cr, researchers used a chitosan-based hydrogel that includes titanate and cellulose nanofibers enhanced with carbon dots (VI). The sorbent's Cr(VI) sorption ability was increased by porous designs, additional titanate, and cellulose nanofibers modified with carbon dots (maximum adsorption capacity, 228.2 mg/g) [153]. A variety of magnetized enhanced chitosan sorbents with core-brush topology were generated by grafting co-polymerization on the surface of chitosan/ $\text{Fe}_3\text{O}_4$  composite particles and utilized to extract two drugs (diclofenac sodium and tetracycline hydrochloride) from water [154]. Method for designing adsorbents based on topological and chemical architectures. Because of the larger surface areas and functionalization, all of improved chitosan sorbents were more efficient at removing contaminants.

Solution casting process was used to create a range of new chitosan/nanodiamond (chitosan/ND) composites with varying surface carboxyl groups and concentrations of NDs. As adsorbent for a model anionic dye, powdery chitosan/ND composites were used (methyl orange, MO). The highest adsorption capability of pure CTS was increased from 167 to 454 mg/g by adding NDs with a high carboxylic content (ND-H) to chitosan, according to experimental data. The extraordinary dye adsorption the oxygen-containing groups on the outer surface of NDs, which would be beneficial for hydrogen bonding and electrostatic interactions with the dye molecules, were connected to the ability on chitosan/ND composites [155].

$\text{CaCO}_3$  was among the most adaptable materials ever devised by man. It's all over the place. accounting for more over 4% of the planet's entire crust. Chalk, marble, and limestone are examples of prevalent  $\text{CaCO}_3$  forms. Bivalves, corals, and snails, among other aquatic biota, have shells are the primary sources of bio-calcium. Aragonite, calcite, and vaterite are the three primary types of carbonates. Though chemically identical, the whiteness, homogeneity, thickness, and purity of various forms differ.  $\text{CaCO}_3$  is widely utilized in the cement industry because of its distinctive white hue. It's also used in applications as a spacer and/or coating pigment, plastics, paints, and paper. In addition, because of its antacid qualities,  $\text{CaCO}_3$  is employed acidic conditions in soil and water in industrial environments.  $\text{CaCO}_3$  helps the environment by treating contaminated water. In tissue bio-engineering, it is commonly employed.  $\text{CaCO}_3$  is abundant in two types of sepia and bivalve shells are two types of marine trash. Shells from the aforementioned aquatic biota function as external and interior bones, protecting the soft parts of bivalve's bodies. SS stands for sepia shells and is a by-product of the fishing industry. Provide predators with mechanical defence. Despite their high calcium content, they are often discarded without being valued commercially. This could result in some local environmental problems, particularly in Egypt's Port Said. Exploiting this waste product for color removal would provide a win-win situation. According to a literature review, color removal with cuttlefish bones has received very little attention [156].

*Anadara uropigimelana* bivalve shells were originally used as a biosorbent for MB recovery from an aqueous solution. Under ideal conditions, 93.6% of the MB was removed (starting pH of 10.4, sorbent dosage of 1 g/L, initial MB

concentration of 20 mg/L, and temperature of 25°C). But at the other hand, bivalve shells, are 95% CaCO<sub>3</sub> with 5% protein and carbohydrate content. It's employed as an adsorbent material for the environment because of its structural and surface qualities.

Pollutants are removed from the environment through a variety of methods. Calcium carbonate compounds are a type of calcium carbonate that can be made in a variety of ways generated immediately by reacting CaCO<sub>3</sub> with a hydrochloric solution is calcium chloride (CaCl<sub>2</sub>). Using wasted eggshells to manufacture vaterite calcium carbonate microparticles, the removal effects and underlying process for a variety of heavy metal ions were studied. Pb(II) (99.9%), Cr(III) (99.5%), Fe(III) (99.3%), and Cu(II) (57.1%) were all removed differently by CaCO<sub>3</sub>. Sepia shells (cuttlefish bones) were used to make a sorbent that was tested for cationic dye (crystal violet, CV) and anionic dye sorption (Congo red, CR). To modify the sorbent, sepia shell powder was mixed with urea in the presence of formaldehyde (SSBC). CV and CR have maximal sorption capacities of 0.536 and 0.359 mmol/g, respectively, at pH 10.6 and 2.4 [157]. SSBC is a software that allows you to connect to the internet. At pH 10.5 and 2.3, maximum sorption capacities for MB and RB5 are 0.794 mmol/g (254.05 mg/g) and 0.271 mmol/g (269.18 mg/g). Biosorbents based on chitosan and alginate had the greatest metal ion elimination sorption capacities when compared to the other biosorbents studied. For cationic dye elimination, one of most powerful sorbents were chitosan-based, whereas, alginate-based sorbents were the most effective. The chemical stability of alginate has been proven. Chitosan composites with cross-linking agents added, on the other hand, could be able to overcome this drawback.

The recycling of these biomasses will, in general, yield several benefits. Its use will contribute to the reduction of waste. Furthermore, pollutant concentrations in various water resources will be reduced. Many environmental issues can be solved this way. Other notable advantages, such as cheap operating and manufacturing costs as well as great efficiency, may be realized. The PSO accurately approximated CV adsorption, whereas the PFO closely matched MO's. The Langmuir adsorption isotherm for CV and MO was closely adsorption equilibrium values were matched. Adsorption efficiency of MB was three times higher with composite beads compared with chitosan beads, and 1.4 times higher with AB 25 [150]. The researchers worked hard to improve chitosan's selectivity for certain metal ions. Grafting 2-mercaptobenzimidazole onto chitosan microparticles, for example, lets extremely selective sorbents to be developed. Magnetite particles are also a key component in making chitosan microparticles easier to use and recover. The sorbent was shown to have a high selectivity for precious metals as compared to base metals (Table 8).

Pollutants are removed from the environment through a variety of methods [158]. Calcium chloride is one of the calcium carbonate compounds that can be made quickly by combining CaCO<sub>3</sub> with a hydrochloric solution (CaCl<sub>2</sub>). Utilizing wasted oyster shells to manufacture vaterite calcium carbonate microparticles, the elimination metal effects and underlying process for a variety of heavy metal ions were studied. CaCO<sub>3</sub> eliminated 99.9% of Pb(II), 99.5%

of Cr(III), 99.3% of Fe(III), and 57.1% of Cu(II) (Lin et al., 2020). Sepia shells (cuttlefish bones) were used to create a sorbent that was tested for cationic dye (crystal violet, CV) and anionic dye sorption (Congo red, CR). To modify the sorbent, sepia shell powder was mixed with urea and formaldehyde (SSBC). Maximum sorption capacities for CV and CR at pH 10.6 and 2.4, respectively, are 0.536 and 0.359 mmol/g [157]. SSBC is a software that allows you to connect to the internet. At pH 10.5 and 2.3, maximum sorption capacities for MB and RB5 are 0.794 mmol/g (254.05 mg/g) and 0.271 mmol/g (269.18 mg/g). With such a maximal absorption rate of 441 mg/g, an environmentally friendly sorbent based on marine brown algae and bivalve shells was recently investigated for subsequent uptake of Congo red dye and copper(II) ions [157]. Biosorbents based on chitosan and alginate had metal ions elimination with the highest sorption capabilities when compared to the other biosorbents studied. For cationic dye elimination, a most powerful substances were chitosan-based sorbents, whereas alginate-based sorbents were the most effective. The chemical stability of alginate has been proven. Cross-linking agents added to chitosan composites, on the other hand, could be able to overcome this drawback.

The recycling of these biomasses will, in general, yield several benefits. Its use will contribute to the reduction of waste. Furthermore, pollutant concentrations in various water resources will be reduced. Many environmental issues can be solved this way. Other notable advantages, such as cheap operating and manufacturing costs as well as great efficiency, may be realized.

## 8. Equilibrium and kinetic modelling

In adsorption research, equilibrium isotherms and kinetic models are critical because they allow for optimal dye adsorption experimental design. There are additional regression analyses displayed. Because linear modelling contradicts the premise that the least squares method is correct, nonlinear modelling is more accurate [166].

The PSO the most appropriate model for dye adsorption kinetics, as shown in Eqs. (1) and (2) show the different types of kinetic pseudo-first-order and pseudo-second-order models, respectively, where  $q_e$  and  $q_t$  (mg/g) are the quantities of colors extracted by the adsorbent at equilibrium and at any time  $t$ , respectively, and  $K_2$  is the pseudo-second-order adsorption model's rate constant (mg/min)(min).

$$\log(q_e - q_t) = \log q_e - \left( \frac{K_1}{2.303} \right) t \quad (1)$$

$$\frac{t}{q_t} = \frac{1}{K_2 q_e^2} + \frac{t}{q_e} \quad (2)$$

Many researchers are interested in pollutant adsorption on adsorbent surfaces, as well as determining which adsorption capability and isotherm models best fit experimental data. Isotherms depict the relationship between the pollutant concentration in solution and the amount of contamination absorbed by the solid phase when both

Table 8  
Different biosorbents' sorption capability and elimination (percentage) are compared

Biosorbent	Contaminant	Biosorption capacity (mg/g)	Mechanism of biosorption	References
Green microalgae <i>Chlorella pyrenoidosa</i>	RB	63.14	Electrostatic interaction	[79]
Sepia shell based composites	Methylene blue	254.05	Electrostatic interaction	[138]
Sepia shell based composites	RB5	269.18	Electrostatic interaction	[138]
Magnetic chitosan glutaraldehyde composite	Crystal violet	105.47	Electrostatic interaction	[159]
ILAC	Reactive blue dye	364.4	Electrostatic interaction	[160]
Ethylenediamine modified fiber obtained from natural <i>Populus tremula</i>	AB 25	67	Van der waals forces $\pi$ - $\pi$ stacking and hydrogen bond	[161]
<i>Carica</i> papaya wood	Malachite green	52.63	Electrostatic interaction	[102]
Grape pomace	KROM KGT dye	180.2	Electrostatic interaction	[162]
Chemically modified masau stones	Orange (II) dye	136.8	Hydrogen bonding and electrostatic interaction	[163]
Millimetre-sized chitosan/carboxymethyl cellulose hollow capsule	Methylene blue	64.6	Electrostatic interaction, complexation, hydrogen bonding and Van der waals forces	[164]
Millimetre-sized chitosan/carboxymethyl cellulose hollow capsule	Acid blue 113 dyes	526.8	Electrostatic interaction, complexation, hydrogen bonding and Van der waals forces	[164]
Date seeds activated carbon (DSAC)	Acid yellow 99	563.07	Chemisorption	[165]
Date seeds activated carbon (DSAC)	Malachite green	91.22	Chemisorption	[165]

phases are in equilibrium and understood in terms of how contaminants are adsorbed. Adsorption isotherms can be used to evaluate the adsorption capacity and the best circumstances for good adsorption. Experimental data are analyzed using the correlation coefficient ( $R^2$ ) to see if they follow isotherm theories. The equilibrium adsorption isotherm investigates the distribution of in between solid adsorbent and the liquid solution adsorbate molecules or ions. Fitting isotherm data to a variety of isotherm models is a useful step that may be used to design the adsorption process and determine the best isotherm model.

The Langmuir and Freundlich isotherm models are given in linear form and are based on the ideal assumptions of monolayer adsorption of adsorbate on the adsorbent surface, where Eq. (3) (linear) and Eq. (4) (non-linear) show the various forms of the isotherm model [167].

$$\frac{C_e}{q_e} = \frac{1}{q_m K_L} + \frac{C_e}{q_m} \quad (3)$$

The monolayer adsorption that occurs at certain homogeneous spots on the adsorbent is represented by the Langmuir isotherm. There is no more adsorption on a site after it has been occupied by a contaminant.

The mechanism of adsorption for the equilibrium isothermal adsorption system, as demonstrated by the adsorption isotherm and kinetic of methylene blue on ZIF-8, is one of the most important pieces of knowledge. Therefore, the most pertinent correlation for the curves of equilibrium needs to

be determined. Four adsorption isotherm models, Langmuir, [168] Freundlich, [169] Dubinin-Radushkevich [170] and Temkin, [171] were helpful in evaluating the experimental effects of adsorption in this study [172].

In order to conduct isothermal adsorption studies at room temperature, 0.02 g of ZIF-8 was added to 25 mL of MB aqueous solution at various concentrations as a starting point in the range  $2.7 \times 10^{-3}$  mol/L to  $2.2 \times 10^{-3}$  mol/L Fig. 11 and Table 8. The equilibrium was then achieved after shaking the solution for 90 min at 110 rpm.

With the proposed chemisorption procedure, the mean energy value of sorption for MB is 15.9 kJ/mol (Fig. 11). The physical separation energy limit (below 8 kJ/mol) and chemical sorption (up to 8 kJ/mol) sorption is usually acknowledged to be 8 kJ/mol. It's assumed (Table 9). Based on their  $R^2$  values, the models are sorted in the following order: For MB, Langmuir > Temkin > Dubinin-Radushkevich > Freundlich > Langmuir > Temkin > Dubinin-Radushkevich > Freundlich.

Further research into the MB adsorption at the adsorbent was conducted in order to understand more about the adsorption properties, which were crucial for the validation of the method's output [175]. The pseudo-first-order and pseudo-second-order kinetic, Weber and Morris, and Elovich equations utilized to analyzed the adsorption findings (Fig. 12). The calculated data is summarized in Table 10 [176,177]. The correlation coefficients demonstrate that the pseudo-second-order kinetic equation was utilized to better understand the adsorption process, demonstrating that chemical adsorption was a rate-controlled process.

Table 9  
Adsorption of MB by ZIF-8 isotherms and their linear forms [173,174]

Isotherm	Equation	Value of parameters	
Langmuir	$\frac{C_e}{q_e} = \frac{1}{q_m K_L} + \frac{C_e}{q_m}$	$q_{m,exp}$ (mmol/g)	1.681
		$q_m$ (mmol/g)	1.686
		$K_L$ (dm <sup>3</sup> /mg)	40,067.56
		$R^2$	0.9995
Freundlich	$\ln q_e = \ln K_F + \frac{1}{n} \ln C_e$	$n$	4.308
		$K_F$ (dm <sup>3</sup> /mg)	10.078
		$R^2$	0.7738
Dubinin–Radushkevich	$\ln q_e = \ln Q_{DR} - K_{DR} \varepsilon^2$	$Q_{DR}$	1.243
		$K_{DR}$	-1.97E-09
		$E_a$	15.9
		$R^2$	0.897
Temkin	$q_e = \beta_T \ln K_T + \beta_T \ln C_e$	$\beta_T$	10,866.54
		$K_T$ (dm <sup>3</sup> /mg)	14.83
		$R^2$	0.948

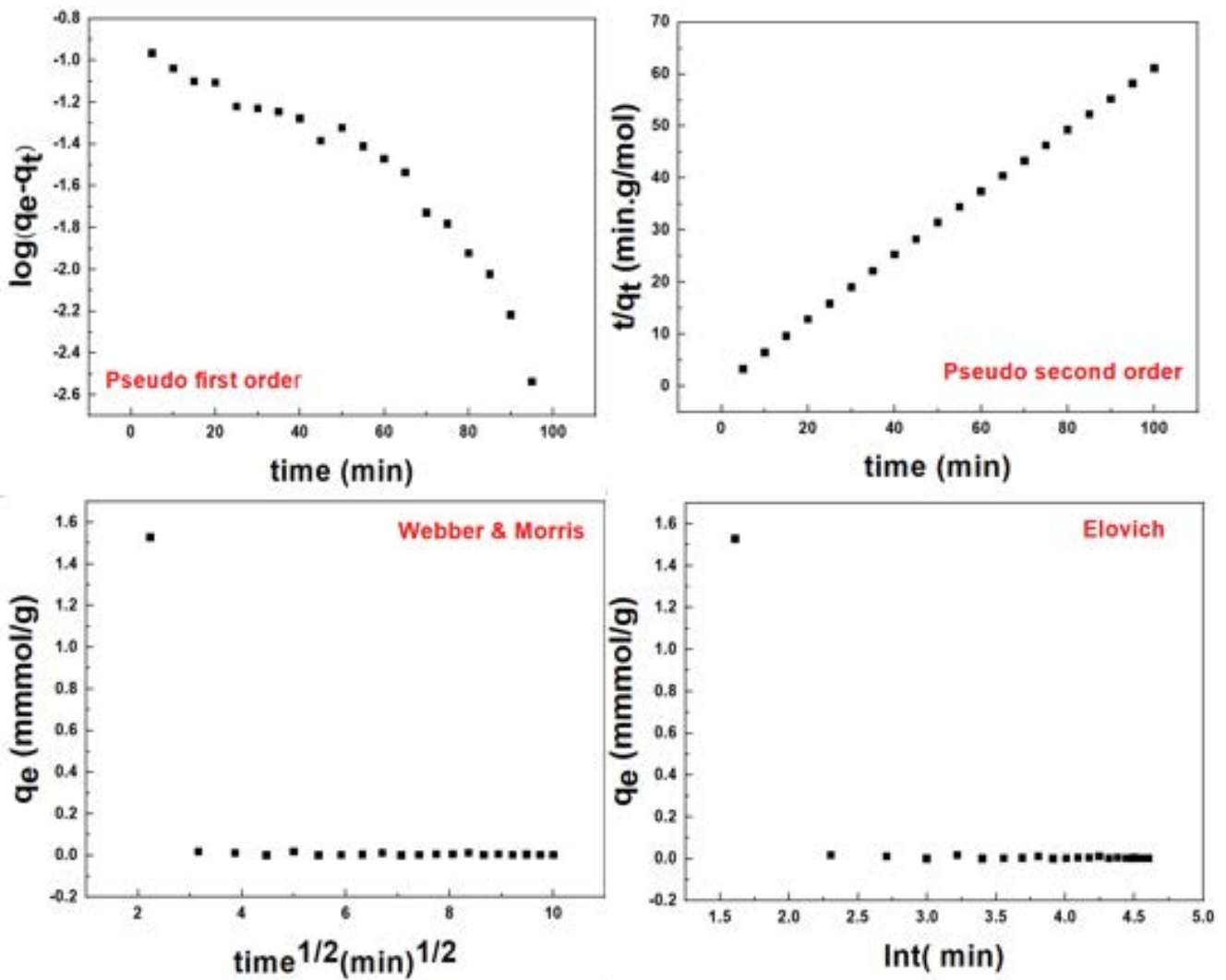


Fig. 12. Linearized plots of adsorption kinetic models of MB at ZIF-8.

Table 10

For the adsorption of MB by ZIF-8, kinetic parameters and their correlation coefficients [173,174]

Model	Equation	Value of parameters	
Pseudo-first-order kinetic	$\log(q_e - q_t) = \log q_e - \left(\frac{K_1}{2.303}\right)t$	$K_1$ (min <sup>-1</sup> )	-0.0144
		$q_e$ (mmol/g)	0.107
		$R^2$	0.88588
Pseudo-second-order kinetic	$\frac{t}{q_t} = \frac{1}{K_2 q_e^2} + \frac{t}{q_e}$	$K_2$ (min <sup>-1</sup> )	0.526
		$q_e$ (mmol/g)	1.645
		$R^2$	0.9998
Intraparticle diffusion	$q_t = K_i t^{1/2} + X$	$K_i$ (mg/g·min <sup>1/2</sup> )	0.00723
		$X$ (mg/g)	0.58
		$R^2$	0.92685
Elovich	$q_t = \frac{1}{\beta} \ln(\alpha\beta) + \frac{1}{\beta} \ln t$	$\beta$ (g/mg)	-3.86
		$\alpha$ (mg/g·min)	2.85
		$R^2$	0.349
Experimental data		$q_{e,exp}$ (mmol/g)	1.635

## 9. Thermodynamic modelling

The describes the overall is significantly influenced by thermodynamic modeling, which includes characteristics such as  $\Delta G$ ,  $\Delta H$  and  $\Delta S$  determining It is an adsorption process in and of itself, regardless about whether the adsorption reaction is endothermic or exothermic. The change in Gibb's free energy ( $\Delta G$ ) is shown in Eq. (4) [178].

$$\Delta G^\circ = \Delta H^\circ - T\Delta S^\circ \quad (4)$$

used a graph to obtain thermodynamic parameters and their values. Because adsorption method exothermic,  $\Delta H^\circ$  value was negative. Negative Gibb's free energy ( $\Delta G$ ) values The spontaneous nature of RhB adsorption on MgO-FCM-NPs, whereas the positive enthalpy ( $H$ ) values of RhB adsorption onto MgO-FCM-NPs illustrates the endothermic character of the process [179]. RBB adsorption on P- $\gamma$ -Fe<sub>2</sub>O<sub>3</sub> was other study discovered it to be non-spontaneous and endothermic.

## 10. Dye adsorption simulation and molecular modelling

For better dye adsorption understanding processes, computational tool would provide additional or alternate data. Removal of colorant from environmental waste, numerous computer chemical technologies used. Density functional theory (DFT) and binitio approaches are the most commonly utilized in dye adsorption molecular simulation research [180]. However, certain experiments the experiments were carried out using numerical simulations and QM/MM (quantum mechanics and molecular mechanics).

The majority of dye adsorption DFT investigations are conducted to obtain additional data in additional to the results of the experiments [180]. DFT-based characteristics like chemical roughness, chemical potential, dipole moment, electrophilicity and nucleophilicity indices, Fukui indices, HOMO and LUMO, or UV-Vis spectra are calculated to analyse the interactions of dyes and adsorbents [180]. The adsorption of three coumarin-based dyes was investigated.

On various collections of TiO<sub>2</sub> using a combined DFT and TD-DFT investigation used both DFT and experimental approaches to the adsorption of two cationic dyes (methylene blue with Basic Yellow). The B3LYP exchange and correlation functionals were used in the DFT investigation, in addition to the 6-31G (d,p) basis set Electrophilicity and nucleophilicity indices of the dyes [181].

Used Bombaxbuonopozense as an adsorbent to study the B3LYP/6-31G was used to bind two cationic dyes (Basic Blue 41 and Basic Yellow 28) (d,p). The chemical hardness index, as well as the electrophilicity and nucleophilicity indices, were used to calculate various DFT descriptors. Estimated solvation free energies, Fukui indices, chemical hardness, and dipole moments at the CAM-B3LYP/6e31G (d,p) theoretical level to investigate the azo dyes dissociation (named blue acid 113, 114, 118, and 120) by oxidation. Demonstrated that the experimental data and the theoretically calculated oxidation mechanism were in good accord. Liu et al. [182] used DFT/LDA-CAPZ and experimental approaches to look into the adsorption properties of Sm<sub>2</sub>CuO<sub>4</sub> for MG. The adsorption energy computed using DFT in this study matched the actual results [182]. DFT simulations were used by Luo et al. [183] to investigate Cucurbit uril adsorption of acidic blue 25. To compare the UV-Vis spectrum with experimental data, the scientists employed the theoretical level of B3LYP/6-31 G (d) and the PCM solvation model.

DFT, in addition to providing complimentary information, it provides alternative information to experimental data the adsorption energy is calculated. The adsorption energy is the binding energy between both the absorbent and the dye. Since it accounts for the interaction between the adsorbent and the dye, it could be used as an indication of sorption strength Haouti et al. [184]. The absorption of crystal violet and toluidine blue onto Na-montmorillonite nano-clay was investigated using molecular dynamics and DFT-based molecular descriptors.

The adsorption energies reveal that crystal violet and toluidine blue can be effectively removed by the Na-montmorillonite nano-clay. Dastgerdi [184] also used

DFT to explore the use of bifunctional carbon nanotubes to remove indigo carmine colour. The PerdewBurkeErnzerh exchange and correlation functional was utilised in combination with the double numeric plus polarization basis set. Functionalization boosts carbon nanotube adsorption capacity, according to the adsorption energies.

Molecular simulations have been used to investigate dye adsorption, numerous computational methodologies have been explored. The majority of the investigations used additional information based on dye DFT descriptors can be obtained using DFT and ab-initio methods. Researchers can use features to predict and explain how the dye will interact with the adsorbent. Despite the fact that these descriptions are useful as used in conjunction with experimental results, they cannot be used alone to describe dye adsorption on adsorbents.

Static DFT studies (or genuine DFT research used for adsorption process) are unable to adequately describe the interaction between dyes (or adsorbates in general) and adsorbents. This is because DFT investigations focused solely on dye interaction with adsorbents, rather than dye connections with the solvent or other molecules in the environment. In rare cases where the interaction between dyes and their surroundings is stronger than the interaction between dyes and the adsorbent, the current DFT results will be null.

Only a few MD simulations are capable of accurately describing dye adsorption. Only certain adsorbents with well-known molecular structures can be used with this method. The structure of the adsorbent is unknown in general (Table 11).

Even though these descriptions are beneficial when used in conjunction with experimental results, they are not sufficient on their own they cannot be used alone to describe dye adsorption on adsorbents.

Static DFT analyses (or genuine DFT research used for dye adsorption) are unable to adequately describe the interaction between dyes (or adsorbates in general) and adsorbents. This is because DFT investigations focused solely on dye interactions with adsorbents, rather than dye interactions with the solvent or other molecules in the environment.

#### 10.1. Active sites

The method of analysing the responsive groups evaluated adsorbate/adsorbents organization and determining

the electrophilic/nucleophilic attack area as well as the electrostatic potential zero areas called as molecular electrostatic potential (MEP) (Fig. 13). MEP were cast-off to map entire MB's electron density surface in this investigation. Different shades were used to indicate the MEP's variables in these maps (red, yellow, green, light blue and blue) (Fig. 14). Similarly, red and yellow colours were used to indicate negative MEP levels, that are connected with electrophilic assault; blue colours were used to indicate positive MEP values, whose are linked with nucleophilic attack; and green was used to indicate the MEP zero area (Fig. 15). As shown in MEP map, the MEP of adsorbate indicates that the adsorbate is more or less susceptible to nucleophilic attack. Furthermore, the MEP map demonstrates that the MEP for the MB adsorbate accepts that the MB is typically prone to nucleophilic attacks (Table 11) [185,186] (Fig. 16).

### 11. Statistical physical modeling

#### 11.1. Adsorption isotherm modeling

Use of The use of theoretical values to correspond equilibrium data is a crucial part of the original design and operation of an adsorption process. Statistical physics methods were used to explain the experimental adsorption data: the monolayer adsorption models coupled with ideal gas (MMIG) (Eq. 5) and the monolayer adsorption model coupled with real gas (MMRG) (Eq. 6). Fitting approach was indeed using nonlinear optimisation depending on the Generalized Reduced Gradient method Microsoft Excel's solver add-in (Microsoft Corporation, 2007). As a result, it was widely believed that the most appropriate model was determined by the magnitude of the correlation coefficient,  $R^2$  as adsorbate molecules can interact with nearby molecules in either an attractive or repellent manner. Based on the surface properties of the adsorption process, these adsorbate interactions may coexist and cause adsorption competition that influences the final findings [187,188].

$$\text{MMIG: } Q_a = \frac{nN_m}{1 + \left(\frac{W}{c}\right)} \quad (5)$$

$$\text{MMRG: } Q_a = \frac{nN_m}{1 + \left(W \frac{1-bC}{C} e^{2\beta C} e^{-\frac{bC}{1-bC}}\right)^n} \quad (6)$$

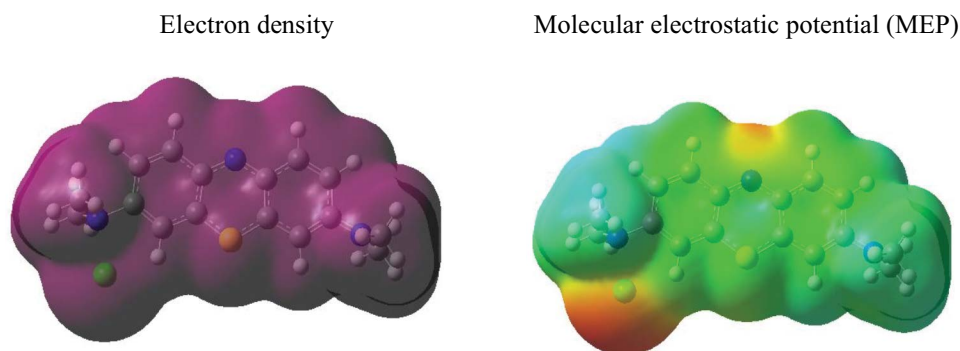


Fig. 13. The whole electron density surfaces is mapped using the electron density molecular electrostatic potential (MEP) for MB.

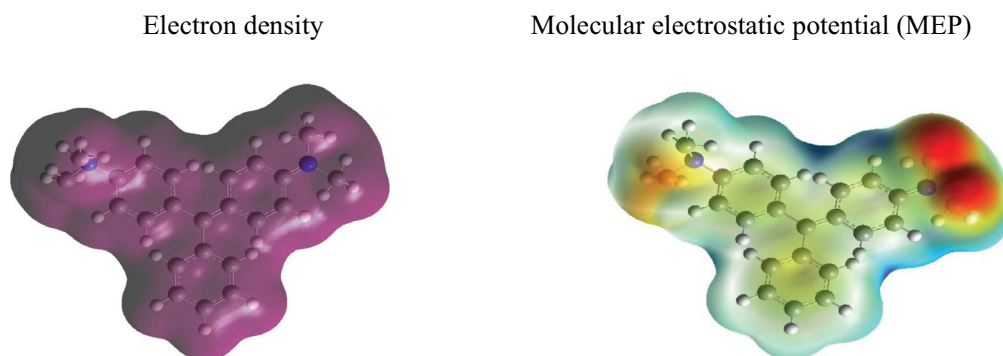


Fig. 14. Total electron density surface mapped with electron density molecular electrostatic potential (MEP) for MG.

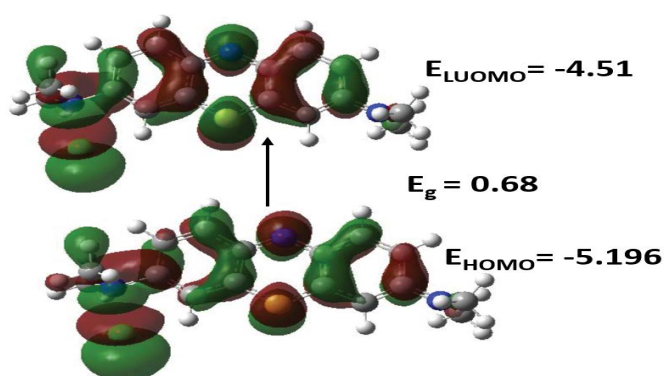


Fig. 15. Molecular orbital density pattern of optimum MB structures at the frontier.

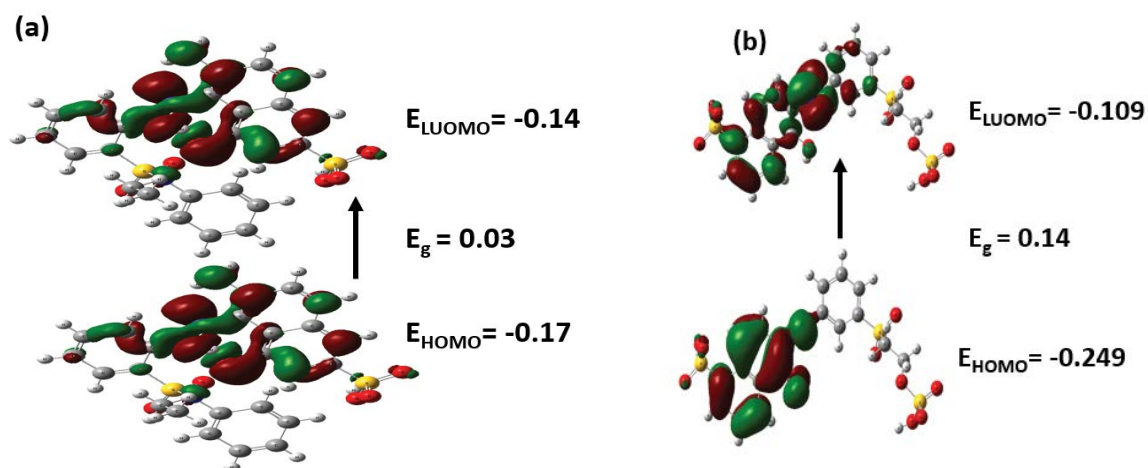


Fig. 16. Optimized structures of frontier molecular orbital density distribution of (a) AR57 and (b) RR.

Table 11  
Quantum chemical parameters computed for the investigated dyes

Comp.	$E_{\text{HOMO}}$ (eV)	$E_{\text{LUMO}}$ (eV)	$\Delta E$ (eV)	$X$ (eV)	$\eta$ (eV)	Pi (eV)	$\sigma$ (eV <sup>-1</sup> )	$S$ (eV <sup>-1</sup> )	$\Omega$ (eV)	$\Delta N_{\text{max}}$
MB	-5.196	-4.51	0.683	4.85	-1.915	-4.9	-0.5	-0.95	-22.56	2.53
AR57	-0.17	-0.13	0.04	0.15	-0.045	-0.15	-22.2	-0.0225	-0.001	3.333
RR	-0.109	-0.249	-0.14	0.179	-0.1945	-0.179	-5.14	-0.0973	-0.003	0.920

### 11.2. Statistical physics characterization

The method to mathematical modelling basis of statistical physics in the gaseous or liquid phase of equilibrium adsorption is a potent technique for characterization during absorption, there are interface effects. The parameter estimates that may be retrieved do have a physical meaning that helps to explain the observable adsorption characteristics. As a consequence, all of the MMRG model's fitting parameters were presented in this paragraph and then investigated to describe and explain the studied adsorption [188].

## 12. Conclusion

This scope the elimination of colours from wastewaters utilizing various adsorbents such as metal oxide, MOF's, alumina, and zeolite are efficient for dyes and wastewater removal. To increase the number of accessible sorption sites and binding functional groups on the produced adsorbent surfaces, a variety of physical and chemical treatments can be used to change biomass porosity and surface areas. The much more commonly reported adsorption methods for the removal of both inorganic and organic dyes include electrostatic contact, ion exchange, and complexation. Despite the great progress in the creation of various biosorbents, there are still several issues connected with these materials, such as pH stability, sorption capacity, and durability, that must be addressed in future applications. Dyes residues in water are causing widespread concern because of the potentially dangerous effects they have on the environment. New generation water contaminants have been discovered to be the cause of the contamination of several water supplies. These developing contaminants have been removed using a variety of new generation nano-adsorbents. Even at low concentrations, that is,  $\mu\text{g/L}$ , these new generation nano-adsorbents may remove new generation contaminants across a range of pH and temperature conditions. These adsorbents only require a little dose, which makes their use cost-effective. Additionally, it is noted that the removal duration, which ranges from 1.0 to 15.0 min, is relatively quick. New generation nano-adsorbents are only occasionally used to remove new generation contaminants. In order to remove new emerging pollutants, even at the trace level, there is a tremendous need to develop more novel and secure new generation nano-adsorbents with higher affinity, capacity, selectivity, and ability to perform under diverse experimental settings.

### Funding

This research received no external funding.

### Declaration of interest

The authors declare that they have no known competing financial interests or personal relationships that could have influenced the work reported in this paper.

### References

- [1] H. Jactel, F. Verheggen, D. Thiéry, A.J. Escobar-Gutiérrez, E. Gachet, N. Desneux, N.W. Group, Alternatives to neonicotinoids, *Environ. Int.*, 129 (2019) 423–429.
- [2] G. Berton, S. Gordon, Modulation of macrophage mannose-specific receptors by cultivation on immobilized zymosan. Effects on superoxide-anion release and phagocytosis, *Immunology*, 49 (1983) 705–715.
- [3] E. Silveira, P.P. Marques, S.S. Silva, J.L. Lima-Filho, A.L.F. Porto, E.B. Tambourgi, Selection of *Pseudomonas* for industrial textile dyes decolorization, *Int. Biodeterior. Biodegrad.*, 63 (2009) 230–235.
- [4] A.Z. El-Sonbati, M.A. Diab, A.A. El-Bindary, M.I. Abou-Dobara, H.A. Seyam, Supramolecular coordination and antimicrobial activities of constructed mixed ligand complexes, *Spectrochim. Acta, Part A*, 104 (2013) 213–221.
- [5] N. Mathur, P. Bhatnagar, P. Bakre, Assessing mutagenicity of textile dyes from Pali (Rajasthan) using Ames bioassay, *Appl. Ecol. Environ. Res.*, 4 (2006) 111–118.
- [6] I. Ali, P. Singh, H.Y. Aboul-Enein, B. Sharma, Chiral analysis of ibuprofen residues in water and sediment, *Anal. Lett.*, 42 (2009) 1747–1760.
- [7] I. Ali, C.K. Jain, Groundwater contamination and health hazards by some of the most commonly used pesticides, *Curr. Sci.*, 75 (1998) 1011–1014.
- [8] A.A. Basheer, Chemical chiral pollution: impact on the society and science and need of the regulations in the 21st century, *Chirality*, 30 (2018) 402–406.
- [9] A.A. Basheer, I. Ali, Stereoselective uptake and degradation of ( $\pm$ )-o, p-DDD pesticide stereoisomers in water-sediment system, *Chirality*, 30 (2018) 1088–1095.
- [10] A.A. Basheer, New generation nano-adsorbents for the removal of emerging contaminants in water, *J. Mol. Liq.*, 261 (2018) 583–593.
- [11] I. Ali, A.A. Basheer, A. Kucherova, N. Memetov, T. Pasko, K. Ovchinnikov, V. Pershin, D. Kuznetsov, E. Galunin, V. Grachev, A. Tkachev, Advances in carbon nanomaterials as lubricants modifiers, *J. Mol. Liq.*, 279 (2019) 251–266.
- [12] I. Ali, O.M.L. Alharbi, Z.A. AlOthman, A. Alwarthan, A.M. Al-Mohaimeed, Preparation of a carboxymethylcellulose-iron composite for uptake of atorvastatin in water, *Int. J. Biol. Macromol.*, 132 (2019) 244–253.
- [13] A.A. Basheer, Advances in the smart materials applications in the aerospace industries, *Aircr. Eng. Aerosp. Technol.*, 92 (2020) 1027–1035.
- [14] I. Ali, A.E. Burakov, A.V. Melezhih, A.V. Babkin, I.V. Burakova, M.E.A. Neskornaya, E.V. Galunin, A.G. Tkachev, D.V. Kuznetsov, Removal of copper(II) and zinc(II) ions in water on a newly synthesized polyhydroquinone/graphene nanocomposite material: kinetics, thermodynamics and mechanism, *ChemistrySelect*, 4 (2019) 12708–12718.
- [15] A. Walters, D. Santillo, P. Johnston, An Overview of Textiles Processing and Related Environmental Concerns, Greenpeace Research Laboratories, Department of Biological Sciences, University of Exeter, Exeter EX4 4PS, UK, 2005.
- [16] N. Hassan, A.Z. El-Sonbati, M.G. El-Desouky, Synthesis, characterization, molecular docking and DNA binding studies of Cu(II), Ni(II), Zn(II) and Mn(II) complexes, *J. Mol. Liq.*, 242 (2017) 293–307.
- [17] I. Ali, S. Afshinb, Y. Poureashgh, A. Azari, Y. Rashtbari, A. Feizizadeh, A. Hamzezhadeh, M. Fazlzadeh, Green preparation of activated carbon from pomegranate peel coated with zero-valent iron nanoparticles (nZVI) and isotherm and kinetic studies of amoxicillin removal in water, *Environ. Sci. Pollut. Res.*, 27 (2020) 36732–36743.
- [18] M. Tanzifi, S.H. Hosseini, A.D. Kiadehi, M. Olazar, K. Karimipour, R. Rezaimehr, I. Ali, Artificial neural network optimization for methyl orange adsorption onto polyaniline nano-adsorbent: kinetic, isotherm and thermodynamic studies, *J. Mol. Liq.*, 244 (2017) 189–200.
- [19] G. McMullan, C. Meehan, A. Conneely, N. Kirby, T. Robinson, P. Nigam, I. Banat, R. Marchant, W. Smyth, Microbial decolorisation and degradation of textile dyes, *Appl. Microbiol. Biotechnol.*, 56 (2001) 81–87.
- [20] A.A. El-Bindary, M.G. El-Desouky, M.A.M. El-Afify, Thermal and spectroscopic studies of some prepared metal complexes and investigation of their potential anticancer

- and antiviral drug activity against SARS-CoV-2 by molecular docking simulation, *Biointerface Res. Appl. Chem.*, 12 (2021) 1053–1075.
- [21] S. El Harfi, A. El Harfi, Classifications, properties and applications of textile dyes: a review, *Appl. J. Environ. Eng. Sci.*, 3 (2017) 311–320.
- [22] S.M. Burkinshaw, D.S. Jeong, T.I. Chun, The coloration of poly(lactic acid) fibres with indigoid dyes: Part 2: wash fastness, *Dyes Pigm.*, 97 (2013) 374–387.
- [23] M.M. Ghoneim, A.Z. El-Sonbati, A.A. El-Bindary, M.A. Diab, L.S. Serag, Polymer complexes. LX. Supramolecular coordination and structures of N(4-(acrylamido)-2-hydroxybenzoic acid) polymer complexes, *Spectrochim. Acta, Part A*, 140 (2015) 111–131.
- [24] Gh.H. Al-Hazmi, M.S. Refatb, M.G. El-Desouky, F.K.M. Wali, A.A. El-Bindary, Effective removal of industrial dye from aqueous solution using mesoporous nickel oxide: a complete batch system evaluation, *Desal. Water Treat.*, 273 (2022) 246–260.
- [25] G.H. Al-Hazmi, A.M.A. Adam, M.G. El-Desouky, A.A. El-Bindary, A.M. Alsuhaibani, M.S. Refat, Efficient adsorption of Rhodamine B using a composite of Fe<sub>3</sub>O<sub>4</sub>@Zif-8: synthesis, characterization, modeling analysis, statistical physics and mechanism of interaction, *Bull. Chem. Soc. Ethiop.*, 37 (2023) 211–229.
- [26] K.Z. Elwakeel, A.A. El-Bindary, A. Ismail, A.M. Morshidy, Sorptive removal of Remazol Brilliant Blue R from aqueous solution by diethylenetriamine functionalized magnetic macro-reticular hybrid material, *RSC Adv.*, 6 (2016) 22395–22410.
- [27] M.A. El-Bindary, A. Shahat, I.M. El-Deen, M.A. Khalil, N. Hassan, Highly efficient metal–organic frameworks for removal of industrial dyes from aqueous solutions, *Desal. Water Treat.*, 274 (2022) 261–277.
- [28] K.Z. Elwakeel, A.A. El-Bindary, A.Z. El-Sonbati, A.R. Hawas, Adsorption of toxic acidic dye from aqueous solution onto diethylenetriamine functionalized magnetic glycidyl methacrylate-N,N'-methylenebisacrylamide, *RSC Adv.*, 6 (2016) 3350–3361.
- [29] R. Anliker, Ecotoxicological assessment of dyes with particular reference to ETAD's activities, *J. Soc. Dyers Colour.*, 95 (1979) 317–326.
- [30] W.O. Olalekan, Theoretical Prediction of Solubility, Reactivity and Degradation Pathways of Selected AZO Disperse Dyes, University of Johannesburg (South Africa), 2019.
- [31] I. Rezić, I. Steffan, ICP-OES determination of metals present in textile materials, *Microchem. J.*, 85 (2007) 46–51.
- [32] R.W. Tennant, J.E. French, J.W. Spalding, Identifying chemical carcinogens and assessing potential risk in short-term bioassays using transgenic mouse models, *Environ. Health Perspect.*, 103 (1995) 942–950.
- [33] Gh.H. Al-Hazmi, M.S. Refat, M.G. El-Desouky, A.A. El-Bindary, Effective adsorption and removal of industrial dye from aqueous solution using mesoporous zinc oxide nanoparticles via metal organic frame work: equilibrium, kinetics and thermodynamic studies, *Desal. Water Treat.*, 272 (2022) 277–289.
- [34] J.A. Page, P.N. Munsing, Occupational Health and the Federal Government: The Wages Are Still Better, *Law and Contemporary Problems*, 38 (1973) 651–668.
- [35] M. Rafatullah, O. Sulaiman, R. Hashim, A. Ahmad, Adsorption of methylene blue on low-cost adsorbents: a review, *J. Hazard. Mater.*, 177 (2010) 70–80.
- [36] S. De Gisi, G. Lofrano, M. Grassi, M. Notarnicola, Characteristics and adsorption capacities of low-cost sorbents for wastewater treatment: a review, *Sustainable Mater. Technol.*, 9 (2016) 10–40.
- [37] M.T. Yagub, T.K. Sen, S. Afroze, H.M. Ang, Dye and its removal from aqueous solution by adsorption: a review, *Adv. Colloid Interface Sci.*, 209 (2014) 172–184.
- [38] O.A. El-Gammal, F.Sh. Mohamed, Gh.N. Rezk, A.A. El-Bindary, Synthesis, characterization, catalytic, DNA binding and antibacterial activities of Co(II), Ni(II) and Cu(II) complexes with new Schiff base ligand, *J. Mol. Liq.*, 326 (2021) 115223, doi: 10.1016/j.molliq.2020.115223.
- [39] H.A. Kiwaan, A.S. El-Mowafy, A.A. El-Bindary, Synthesis, spectral characterization, DNA binding, catalytic and in vitro cytotoxicity of some metal complexes, *J. Mol. Liq.*, 326 (2021) 115381, doi: 10.1016/j.molliq.2021.115381.
- [40] A.B. dos Santos, F.J. Cervantes, J.B. van Lier, Review paper on current technologies for decolorisation of textile wastewaters: perspectives for anaerobic biotechnology, *Bioresour. Technol.*, 98 (2007) 2369–2385.
- [41] M.B. Kasiri, N. Modirshahla, H. Mansouri, Decolorization of organic dye solution by ozonation; optimization with response surface methodology, *Int. J. Ind. Chem.*, 4 (2013) 3, doi: 10.1186/2228-5547-4-3.
- [42] S. Dawood, T. Sen, Review on dye removal from its aqueous solution into alternative cost effective and non-conventional adsorbents, *J. Chem. Process Eng.*, 1 (2014) 1–11.
- [43] R. Pelegrini, P. Peralta-Zamora, A.R. de Andrade, J. Reyes, N. Durán, Electrochemically assisted photocatalytic degradation of reactive dyes, *Appl. Catal., B*, 22 (1999) 83–90.
- [44] Ü.B. Ögütveren, S. Kopal, Color removal from textile effluents by electrochemical destruction, *J. Environ. Sci. Health. Part A Environ. Sci. Health Part A Environ. Sci. Eng.*, 29 (1994) 1–16.
- [45] M.A.M. Salleh, D.K. Mahmoud, W.A.W.A. Karim, A. Idris, Cationic and anionic dye adsorption by agricultural solid wastes: a comprehensive review, *Desalination*, 280 (2011) 1–13.
- [46] A. Mishra, M. Bajpai, The flocculation performance of *Tamarindus* mucilage in relation to removal of vat and direct dyes, *Bioresour. Technol.*, 97 (2006) 1055–1059.
- [47] Y. Zhou, Z. Liang, Y. Wang, Decolorization and COD removal of secondary yeast wastewater effluents by coagulation using aluminum sulfate, *Desalination*, 225 (2008) 301–311.
- [48] V.K. Gupta, R. Jain, S. Varshney, Electrochemical removal of the hazardous dye Reactofix Red 3 BFN from industrial effluents, *J. Colloid Interface Sci.*, 312 (2007) 292–296.
- [49] A. Aguedach, S. Brosillon, J. Morvan, E.K. Lhadi, Photocatalytic degradation of azo-dyes reactive black 5 and reactive yellow 145 in water over a newly deposited titanium dioxide, *Appl. Catal., B*, 57 (2005) 55–62.
- [50] A.M. Faouzi, B. Nasr, G. Abdellatif, Electrochemical degradation of anthraquinone dye Alizarin Red S by anodic oxidation on boron-doped diamond, *Dyes Pigm.*, 73 (2007) 86–89.
- [51] B.E. Barragán, C. Costa, M. Carmen Márquez, Biodegradation of azo dyes by bacteria inoculated on solid media, *Dyes Pigm.*, 75 (2007) 73–81.
- [52] J. Hardcastle, R.J. McKeown, R. Compton, The 20 kHz sonochemical degradation of trace cyanide and dye stuffs in aqueous media, *New J. Chem.*, 23 (1999) 845–849.
- [53] C. Frijters, R. Vos, G. Scheffer, R. Mulder, Decolorizing and detoxifying textile wastewater, containing both soluble and insoluble dyes, in a full scale combined anaerobic/aerobic system, *Water Res.*, 40 (2006) 1249–1257.
- [54] N.K. Pazarlioglu, R.O. Urek, F. Ergun, Biodecolourization of Direct Blue 15 by immobilized *Phanerochaete chrysosporium*, *Process Biochem.*, 40 (2005) 1923–1929.
- [55] R. Sani, U. Banerjee, Decolorization of Acid Green 20, a textile dye by white rot fungus, *Phanerochaete chrysosporium* in low cost medium, *Adv. Environ. Res.*, 2 (1999) 485–495.
- [56] C.J. Ogugbue, F. Akubenyi, A.A. Ibiene, Bacterial decolorization of acid orange 10 in synthetic wastewater under saline conditions: effect of process parameters, *Singapore J. Sci. Res.*, 2 (2012) 1–13.
- [57] D. Brown, P. Laboureur, The degradation of dyestuffs: part I primary biodegradation under anaerobic conditions, *Chemosphere*, 12 (1983) 397–404.
- [58] A. Stolz, Basic and applied aspects in the microbial degradation of azo dyes, *Appl. Microbiol. Biotechnol.*, 56 (2001) 69–80.
- [59] K.S. Abou-Melha, G.A.A. Al-Hazmi, I. Althagafi, R. Shah, F. Shaaban, N.M. El-Metwaly, A.A. El-Bindary, Preparation of CuO nanoparticles via organometallic chelate for the removal of acid red 57 from aqueous solutions, *Desal. Water Treat.*, 222 (2021) 282–294.
- [60] F.I. El-Dossoki, T.M. Atwee, A.M. Hamada, A.A. El-Bindary, Photocatalytic degradation of Remazol red B and Rhodamine

- B dyes using TiO<sub>2</sub> nanomaterial: estimation of the effective operating parameters, *Desal. Water Treat.*, 233 (2021) 319–330.
- [61] M.D. LeVan, G. Carta, C.M.J.E. Yon, Adsorption and ion exchange, *Energy*, 16 (1997) 17.
- [62] H. Jézéquel, K.H. Chu, Removal of arsenate from aqueous solution by adsorption onto titanium dioxide nanoparticles, *J. Environ. Sci. Health. Part A Toxic/Hazard. Subst. Environ. Eng.*, 41 (2006) 1519–1528.
- [63] S. Mukherjee, S. Kumar, A.K. Misra, M. Fan, Removal of phenols from water environment by activated carbon, bagasse ash and wood charcoal, *Chem. Eng. J.*, 129 (2007) 133–142.
- [64] M.G. El-Desouky, M. Abd El-Wahab, A.A. El-Bindary, Interpretations and DFT calculations for polypropylene/copper oxide nanosphere, *Biointerface Res. Appl. Chem.*, 12 (2022) 1134–1147.
- [65] T.K. Chaithanya, S. Yedla, Adsorption of hexa-valent chromium using treated wood charcoal – elucidation of rate-limiting process, *Environ. Technol.*, 31 (2010) 1495–1505.
- [66] C. Kemball, Physical and chemical aspects of adsorbents and catalysts, *Phys. Bull.*, 21 (1970) 559, doi: 10.1088/0031-9112/21/12/035.
- [67] N. Hassan, A. Shahat, I. El-Deen, M. El-Afify, M.J.J.o.M.S. El-Bindary, Synthesis and characterization of NH<sub>2</sub>-MIL-88 (Fe) for efficient adsorption of dyes, 1258 (2022) 132662.
- [68] D. Caputo, F. Pepe, Experiments and data processing of ion exchange equilibria involving Italian natural zeolites: a review, *Microporous Mesoporous Mater.*, 105 (2007) 222–231.
- [69] M.O. Adebajo, R.L. Frost, J.T. Klopogge, O. Carmody, S. Kokot, Porous materials for oil spill cleanup: a review of synthesis and absorbing properties, *J. Porous Mater.*, 10 (2003) 159–170.
- [70] A.A. El-Bindary, Z. Anwar, T. El-Shafaie, Effect of silicon dioxide nanoparticles on the assessment of quercetin flavonoid using Rhodamine B Isothiocyanate dye, *J. Mol. Liq.*, 323 (2021) 114607, doi: 10.1016/j.molliq.2020.114607.
- [71] A.A. El-Bindary, M.A. Diab, M.A. Hussien, A.Z. El-Sonbati, A.M. Eessa, Adsorption of Acid red 57 from aqueous solutions onto polyacrylonitrile/activated carbon composite, *Spectrochim. Acta, Part A*, 124 (2014) 70–77.
- [72] P. Carrott, M.R. Carrott, P. Mourao, R. Lima, Preparation of activated carbons from cork by physical activation in carbon dioxide, *Adsorpt. Sci. Technol.*, 21 (2003) 669–681.
- [73] R.C. Bansal, J. Donnet, F. Stoeckli, *Active Carbon*, Marcel Dekker, J. Inc., New York, 1988.
- [74] C. Decker, H.L. Xuan, T.N.T. Viet, Photocrosslinking of functionalized rubber. III. Polymerization of multifunctional monomers in epoxidized liquid natural rubber, *J. Polym. Sci., Part A: Polym. Chem.*, 34 (1996) 1771–1781.
- [75] C. Luo, J. Wang, P. Jia, Y. Liu, J. An, B. Cao, K. Pan, Hierarchically structured polyacrylonitrile nanofiber mat as highly efficient lead adsorbent for water treatment, *Chem. Eng. J.*, 262 (2015) 775–784.
- [76] D. Zhao, D.J. Timmons, D. Yuan, H.-C. Zhou, Tuning the topology and functionality of metal–organic frameworks by ligand design, *Acc. Chem. Res.*, 44 (2011) 123–133.
- [77] S.K. Henninger, H.A. Habib, C. Janiak, MOFs as adsorbents for low temperature heating and cooling applications, *J. Am. Ceram. Soc.*, 131 (2009) 2776–2777.
- [78] G.A.A. Al-Hazmi, A.A. El-Zahhar, M.G. El-Desouky, M.A. El-Bindary, A.A. El-Bindary, Efficiency of Fe<sub>3</sub>O<sub>4</sub>@ZIF-8 for the removal of Doxorubicin from aqueous solutions: equilibrium, kinetics and thermodynamic studies, *Environ. Technol.*, (2022) 1–20, doi: 10.1080/09593330.2022.2121181.
- [79] S. Ziane, F. Bessaha, K. Marouf-Khelifa, A. Khelifa, Single and binary adsorption of Reactive black 5 and Congo red on modified dolomite: performance and mechanism, *J. Mol. Liq.*, 249 (2018) 1245–1253.
- [80] V.S. Munagapati, V. Yarramuthi, Y. Kim, K.M. Lee, D.-S. Kim, Removal of anionic dyes (Reactive black 5 and Congo red) from aqueous solutions using banana peel powder as an adsorbent, *Ecotoxicol. Environ. Saf.*, 148 (2018) 601–607.
- [81] T.V. Kumar, V. Sivasankar, N. Fayoud, H. Abou Oualid, A.K. Sundramoorthy, Synthesis and characterization of coral-like hierarchical MgO incorporated fly ash composite for the effective adsorption of azo dye from aqueous solution, *Appl. Surf. Sci.*, 449 (2018) 719–728.
- [82] F.E. García, J. Plaza-Cazón, V.N. Montesinos, E.R. Donati, M.I. Litter, Combined strategy for removal of Reactive Black 5 by biomass sorption on *Macrocystis pyrifera* and zerovalent iron nanoparticles, *J. Environ. Manage.*, 207 (2018) 70–79.
- [83] M. Chang, Y.-h. Shih, Synthesis and application of magnetic iron oxide nanoparticles on the removal of Reactive Black 5: reaction mechanism, temperature and pH effects, *J. Environ. Manage.*, 224 (2018) 235–242.
- [84] X.-J. Jia, J. Wang, J. Wu, W. Teng, B. Zhao, H. Li, Y. Du, Facile synthesis of MoO<sub>3</sub>/CaSO<sub>4</sub> composites as highly efficient adsorbents for Congo red and Rhodamine B, *RSC Adv.*, 8 (2018) 1621–1631.
- [85] H. Chen, S. Wageh, A.A. Al-Ghamdi, H. Wang, J. Yu, C. Jiang, Hierarchical C/NiO-ZnO nanocomposite fibers with enhanced adsorption capacity for Congo red, *J. Colloid Interface Sci.*, 537 (2019) 736–745.
- [86] S.G. Nasab, A. Semnani, A. Teimouri, H. Kahkesh, T.M. Isfahani, S. Habibollahi, Removal of Congo red from aqueous solution by hydroxyapatite nanoparticles loaded on zein as an efficient and green adsorbent: response surface methodology and artificial neural network-genetic algorithm, *J. Polym. Environ.*, 26 (2018) 3677–3697.
- [87] S.-L. Chan, Y.P. Tan, A.H. Abdullah, S.-T. Ong, Equilibrium, kinetic and thermodynamic studies of a new potential biosorbent for the removal of Basic Blue 3 and Congo red dyes: pineapple (*Ananas comosus*) plant stem, *J. Taiwan Inst. Chem. Eng.*, 61 (2016) 306–315.
- [88] S. Wong, N. Abd Ghafar, N. Ngadi, F.A. Razmi, I.M. Inuwa, R. Mat, N.A.S. Amin, Effective removal of anionic textile dyes using adsorbent synthesized from coffee waste, *Sci. Rep.*, 10 (2020) 1–13.
- [89] M.G. El-Desouky, M.A. El-Bindary, A.A. El-Bindary, Effective adsorptive removal of anionic dyes from aqueous solution, *Vietnam J. Chem.*, 59 (2021) 341–361.
- [90] E. Haque, J.W. Jun, S.H. Jhung, Adsorptive removal of methyl orange and methylene blue from aqueous solution with a metal–organic framework material, iron terephthalate (MOF-235), *J. Hazard. Mater.*, 185 (2011) 507–511.
- [91] Uma, S. Banerjee, Y.C. Sharma, Equilibrium and kinetic studies for removal of malachite green from aqueous solution by a low cost activated carbon, *J. Ind. Eng. Chem.*, 19 (2013) 1099–1105.
- [92] I.D. Mall, V.C. Srivastava, N.K. Agarwal, I.M. Mishra, Adsorptive removal of malachite green dye from aqueous solution by bagasse fly ash and activated carbon-kinetic study and equilibrium isotherm analyses, *Colloids Surf., A*, 264 (2005) 17–28.
- [93] P. Janoš, Sorption of basic dyes onto iron humate, *Environ. Sci. Technol.*, 37 (2003) 5792–5798.
- [94] M.S. Derakhshan, O. Moradi, The study of thermodynamics and kinetics methyl orange and malachite green by SWCNTs, SWCNT-COOH and SWCNT-NH<sub>2</sub> as adsorbents from aqueous solution, *J. Ind. Eng. Chem.*, 20 (2014) 3186–3194.
- [95] M. Rajabi, K. Mahanpoor, O. Moradi, Removal of dye molecules from aqueous solution by carbon nanotubes and carbon nanotube functional groups: critical review, *RSC Adv.*, 7 (2017) 47083–47090.
- [96] S. Tahir, N. Rauf, Removal of a cationic dye from aqueous solutions by adsorption onto bentonite clay, *Chemosphere*, 63 (2006) 1842–1848.
- [97] M.J. Iqbal, M.N. Ashiq, Adsorption of dyes from aqueous solutions on activated charcoal, *J. Hazard. Mater.*, 139 (2007) 57–66.
- [98] N. Hassan, A. Shahat, A. El-Didamony, M.G. El-Desouky, A.A. El-Bindary, Synthesis and characterization of ZnO nanoparticles via zeolitic imidazolate framework-8 and its

- application for removal of dyes, *J. Mol. Struct.*, 1210 (2020) 128029, doi: 10.1016/j.molstruc.2020.128029.
- [99] S.U. Ilyas, R. Pendyala, N. Marneni, Stability and agglomeration of alumina nanoparticles in ethanol-water mixtures, *Procedia Eng.*, 148 (2016) 290–297.
- [100] H.R. Pant, H.J. Kim, M.K. Joshi, B. Pant, C.H. Park, J.I. Kim, K. Hui, C.S. Kim, One-step fabrication of multifunctional composite polyurethane spider-web-like nanofibrous membrane for water purification, *J. Hazard. Mater.*, 264 (2014) 25–33.
- [101] J. Yan, Y. Huang, Y.-E. Miao, W.W. Tjiu, T. Liu, Polydopamine-coated electrospun poly(vinyl alcohol)/poly(acrylic acid) membranes as efficient dye adsorbent with good recyclability, *J. Hazard. Mater.*, 283 (2015) 730–739.
- [102] F. Şen, Ö. Demirbaş, M.H. Çalimli, A. Aygün, M.H. Alma, K.S. Nas, The dye removal from aqueous solution using polymer composite films, *Appl. Water Sci.*, 8 (2018) 1–9.
- [103] A. Gouthaman, R.S. Azarudeen, A. Gnanaprakasam, V. Sivakumar, M. Thirumarimurugan, Polymeric nanocomposites for the removal of Acid red 52 dye from aqueous solutions: synthesis, characterization, kinetic and isotherm studies, *Ecotoxicol. Environ. Saf.*, 160 (2018) 42–51.
- [104] M. Mohammadikish, D. Jahanshiri, Rapid adsorption of cationic and anionic dyes from aqueous solution via metal-based coordination polymers nanoparticles, *Solid State Sci.*, 99 (2020) 106063, doi: 10.1016/j.solidstatesciences.2019.106063.
- [105] M.G. El-Desouky, A.A. El-Bindary, M.A. El-Bindary, Low-temperature adsorption study of carbon dioxide on porous magnetite nanospheres iron oxide, *Biointerface Res. Appl. Chem.*, 12 (2021) 6252–6268.
- [106] M. Zhao, P. Liu, Adsorption behavior of methylene blue on halloysite nanotubes, *Microporous Mesoporous Mater.*, 112 (2008) 419–424.
- [107] A. Mittal, J. Mittal, A. Malviya, D. Kaur, V. Gupta, Decoloration treatment of a hazardous triarylmethane dye, Light Green SF (Yellowish) by waste material adsorbents, *J. Colloid Interface Sci.*, 342 (2010) 518–527.
- [108] C.-H. Wu, Adsorption of reactive dye onto carbon nanotubes: equilibrium, kinetics and thermodynamics, *J. Hazard. Mater.*, 144 (2007) 93–100.
- [109] H.I. Dawood, K.S. Mohammed, M.Y. Rajab, Advantages of the green solid state FSW over the conventional GMAW process, *Adv. Mater. Sci. Eng.*, 2014 (2014) 105713, doi: 10.1155/2014/105713.
- [110] S. Kumar, G. Bhanjana, K. Jangra, N. Dilbaghi, A. Umar, Utilization of carbon nanotubes for the removal of rhodamine B dye from aqueous solutions, *J. Nanosci. Nanotechnol.*, 14 (2014) 4331–4336.
- [111] D.P. Dutta, R. Venugopalan, S. Chopade, Manipulating carbon nanotubes for efficient removal of both cationic and anionic dyes from wastewater, *ChemistrySelect*, 2 (2017) 3878–3888.
- [112] L. Lou, R.J. Kendall, E. Smith, S.S. Ramkumar, Functional PVDF/rGO/TiO<sub>2</sub> nanofiber webs for the removal of oil from water, *Polymer*, 186 (2020) 122028, doi: 10.1016/j.polymer.2019.122028.
- [113] G. Singh, D. Rana, T. Matsuura, S. Ramakrishna, R.M. Narbaitz, S. Tabe, Removal of disinfection by-products from water by carbonized electrospun nanofibrous membranes, *Sep. Purif. Technol.*, 74 (2010) 202–212.
- [114] A.S. Ibupoto, U.A. Qureshi, F. Ahmed, Z. Khatri, M. Khatri, M. Maqsood, R.Z. Brohi, I.S. Kim, Reusable carbon nanofibers for efficient removal of methylene blue from aqueous solution, *Chem. Eng. Res. Des.*, 136 (2018) 744–752.
- [115] J. Cheng, C. Zhan, J. Wu, Z. Cui, J. Si, Q. Wang, X. Peng, L.-S. Turng, Highly efficient removal of methylene blue dye from an aqueous solution using cellulose acetate nanofibrous membranes modified by polydopamine, *ACS Omega*, 5 (2020) 5389–5400.
- [116] G.H. Al-Hazmi, M.G. El-Desouky, A.A. El-Bindary, Synthesis, characterization and microstructural evaluation of ZnO nanoparticles by William–Hall and size-strain plot methods, *Bull. Chem. Soc. Ethiop.*, 36 (2022) 815–829.
- [117] B.M. Thamer, H. El-Hamshary, S.S. Al-Deyab, M.H. El-Newehy, Functionalized electrospun carbon nanofibers for removal of cationic dye, *Arabian J. Chem.*, 12 (2019) 747–759.
- [118] Z. Wu, I.-S. Ahn, C.-H. Lee, J.-H. Kim, Y.G. Shul, K. Lee, Enhancing the organic dye adsorption on porous xerogels, *Colloids Surf., A*, 240 (2004) 157–164.
- [119] G.A.A. Al-Hazmi, A.A. El-Zahhar, M.G. El-Desouky, M.A. El-Bindary, A.A. El-Bindary, Adsorption of industrial dye onto a zirconium metal-organic framework: synthesis, characterization, kinetics, thermodynamics, and DFT calculations, *J. Coord. Chem.*, 75 (2022) 1203–1229.
- [120] G. Guzel Kaya, E. Yilmaz, H. Deveci, A novel silica xerogel synthesized from volcanic tuff as an adsorbent for high-efficient removal of methylene blue: parameter optimization using Taguchi experimental design, *J. Chem. Technol. Biotechnol.*, 94 (2019) 2729–2737.
- [121] H. Han, W. Wei, Z. Jiang, J. Lu, J. Zhu, J. Xie, Removal of cationic dyes from aqueous solution by adsorption onto hydrophobic/hydrophilic silica aerogel, *Colloids Surf., A*, 509 (2016) 539–549.
- [122] A. İşildar, E.D. van Hullebusch, M. Lenz, G. Du Laing, A. Marra, A. Cesaro, S. Panda, A. Akcil, M.A. Cucuker, K. Kuchta, Biotechnological strategies for the recovery of valuable and critical raw materials from waste electrical and electronic equipment (WEEE) – a review, *J. Hazard. Mater.*, 362 (2019) 467–481.
- [123] V. Krstić, T. Urošević, B. Pešovski, A review on adsorbents for treatment of water and wastewaters containing copper ions, *Chem. Eng. Sci.*, 192 (2018) 273–287.
- [124] G.A.A. Al-Hazmi, M.A. El-Bindary, M.G. El-Desouky, A.A. El-Bindary, Efficient adsorptive removal of industrial dye from aqueous solution by synthesized zeolitic imidazolate framework-8 loaded date seed activated carbon and statistical physics modeling, *Desal. Water Treat.*, 258 (2022) 85–103.
- [125] M. Fomina, G.M. Gadd, Biosorption: current perspectives on concept, definition and application, *Bioresour. Technol.*, 160 (2014) 3–14.
- [126] M.G. El-Desouky, A.A. El-Bindary, M.A.M. El-Afify, N. Hassan, Synthesis, characterization, theoretical calculation, DNA binding, molecular docking, anticovid-19 and anticancer chelation studies of some transition metal complexes, *Inorg. Nano-Metal Chem.*, 52 (2022) 1–16.
- [127] K.Z. Elwakeel, H.A. El-Sadik, A. Abdel-Razek, M.S. Beheary, Environmental remediation of thorium(IV) from aqueous medium onto *Cellulosimicrobium cellulans* isolated from radioactive wastewater, *Desal. Water Treat.*, 46 (2012) 1–9.
- [128] K.Z. Elwakeel, Environmental application of chitosan resins for the treatment of water and wastewater: a review, *J. Dispersion Sci. Technol.*, 31 (2010) 273–288.
- [129] T.A. Altalhi, M.M. Ibrahim, G.A.M. Mersal, M.H.H. Mahmoud, T. Kumeria, M.G. El-Desouky, A.A. El-Bindary, M.A. El-Bindary, Adsorption of doxorubicin hydrochloride onto thermally treated green adsorbent: equilibrium, kinetic and thermodynamic studies, *J. Mol. Struct.*, 1263 (2022) 133160, doi: 10.1016/j.molstruc.2022.133160.
- [130] N.K. Gupta, A. Gupta, P. Ramteke, H. Sahoo, A. Sengupta, Biosorption-a green method for the preconcentration of rare earth elements (REEs) from waste solutions: a review, *J. Mol. Liq.*, 274 (2019) 148–164.
- [131] I. Hespanhol, A. Prost, WHO guidelines and national standards for reuse and water quality, *Water Res.*, 28 (1994) 119–124.
- [132] S. Lei, Y. Shi, Y. Qiu, L. Che, C. Xue, Performance and mechanisms of emerging animal-derived biochars for immobilization of heavy metals, *Sci. Total Environ.*, 646 (2019) 1281–1289.
- [133] K.Z. Elwakeel, G.O. El-Sayed, S.M. Abo El-Nassr, Removal of ferrous and manganous from water by activated carbon obtained from sugarcane bagasse, *Desal. Water Treat.*, 55 (2015) 471–483.
- [134] X. Qi, R. Liu, M. Chen, Z. Li, T. Qin, Y. Qian, S. Zhao, M. Liu, Q. Zeng, J. Shen, Removal of copper ions from water using

- polysaccharide-constructed hydrogels, *Carbohydr. Polym.*, 209 (2019) 101–110.
- [135] F. Afshariani, A. Roosta, Experimental study and mathematical modeling of biosorption of methylene blue from aqueous solution in a packed bed of microalgae *Scenedesmus*, *J. Cleaner Prod.*, 225 (2019) 133–142.
- [136] E. Daneshvar, A. Vazirzadeh, A. Niazi, M. Sillanpää, A. Bhatnagar, A comparative study of methylene blue biosorption using different modified brown, red and green macroalgae – effect of pretreatment, *Chem. Eng. J.*, 307 (2017) 435–446.
- [137] A.L.D. da Rosa, E. Carissimi, G.L. Dotto, H. Sander, L.A. Feris, Biosorption of rhodamine B dye from dyeing stones effluents using the green microalgae *Chlorella pyrenoidosa*, *J. Cleaner Prod.*, 198 (2018) 1302–1310.
- [138] A.M. Elgarahy, K.Z. Elwakeel, G.A. Elshoubaky, S.H. Mohammad, Microwave-accelerated sorption of cationic dyes onto green marine algal biomass, *Environ. Sci. Technol.*, 26 (2019) 22704–22722.
- [139] S. Rangabhashiyam, E. Suganya, A.V. Lity, N. Selvaraju, Equilibrium and kinetics studies of hexavalent chromium biosorption on a novel green macroalgae *Enteromorpha* sp., *Res. Chem. Intermed.*, 42 (2016) 1275–1294.
- [140] M.A. El-Bindary, M.G. El-Desouky, A.A. El-Bindary, Metal-organic frameworks encapsulated with an anticancer compound as drug delivery system: synthesis, characterization, antioxidant, anticancer, antibacterial and molecular docking investigation, *Appl. Organomet. Chem.*, 36 (2022) e6660, doi: 10.1002/aoc.6660.
- [141] P.S. Saravana, Y.-N. Cho, H.-C. Woo, B.-S. Chun, Green and efficient extraction of polysaccharides from brown seaweed by adding deep eutectic solvent in subcritical water hydrolysis, *J. Cleaner Prod.*, 198 (2018) 1474–1484.
- [142] A.M. Elgarahy, K.Z. Elwakeel, A. Akhdhar, M.F. Hamza, Recent advances in green synthesized nanoengineered materials for water/wastewater remediation: an overview, *Nanotechnol. Environ. Eng.*, 6 (2021) 1–24.
- [143] N. Bordoloi, R. Goswami, M. Kumar, R. Katak, Biosorption of Co(II) from aqueous solution using algal biochar: kinetics and isotherm studies, *Bioresour. Technol.*, 244 (2017) 1465–1469.
- [144] C. Liu, J. Ye, Y. Lin, J. Wu, G.W. Price, D. Burton, Y. Wang, Removal of cadmium(II) using water hyacinth (*Eichhornia crassipes*) biochar alginate beads in aqueous solutions, *Environ. Pollut.*, 264 (2020) 114785, doi: 10.1016/j.envpol.2020.114785.
- [145] X. Hu, L. Long, T. Gong, J. Zhang, J. Yan, Y. Xue, Enhanced alginate-based microsphere with the pore-forming agent for efficient removal of Cu(II), *Chemosphere*, 240 (2020) 124860, doi: 10.1016/j.chemosphere.2019.124860.
- [146] Y. Wei, K.A. Salih, K. Rabie, K.Z. Elwakeel, Y.E. Zayed, M.F. Hamza, E. Guibal, Development of phosphoryl-functionalized algal-PEI beads for the sorption of Nd(III) and Mo(VI) from aqueous solutions – application for rare earth recovery from acid leachates, *Chem. Eng. J.*, 412 (2021) 127399, doi: 10.1016/j.cej.2020.127399.
- [147] M.G. El-Desouky, A.A. El-Bindary, Magnetic metal-organic framework (Fe<sub>3</sub>O<sub>4</sub>@ZIF-8) nanocomposites for adsorption of anionic dyes from wastewater, *Inorg. Nano-Metal Chem.*, (2021) 1–15, doi: 10.1080/24701556.2021.2007131.
- [148] T. Józwiak, U. Filipkowska, Sorption kinetics and isotherm studies of a Reactive Black 5 dye on chitosan hydrogel beads modified with various ionic and covalent cross-linking agents, *J. Environ. Chem. Eng.*, 8 (2020) 103564, doi: 10.1016/j.jece.2019.103564.
- [149] M. Jabli, Synthesis, characterization, and assessment of cationic and anionic dye adsorption performance of functionalized silica immobilized chitosan bio-polymer, *Int. J. Biol. Macromol.*, 153 (2020) 305–316.
- [150] B. Li, Z. Ren, Superior adsorption of direct dye from aqueous solution by Y(III)-chitosan-doped fly ash composite as low-cost adsorbent, *J. Polym. Environ.*, 28 (2020) 1811–1821.
- [151] K.Z. Elwakeel, A.S. Al-Bogami, E. Guibal, 2-Mercaptobenzimidazole derivative of chitosan for silver sorption – contribution of magnetite incorporation and sonication effects on enhanced metal recovery, *Chem. Eng. J.*, 403 (2021) 126265, doi: 10.1016/j.cej.2020.126265.
- [152] J. Weißpflog, A. Gündel, D. Vehlow, C. Steinbach, M. Müller, R. Boldt, S. Schwarz, D. Schwarz, Solubility and selectivity effects of the anion on the adsorption of different heavy metal ions onto chitosan, *Molecules*, 25 (2020) 2482, doi: 10.3390/molecules25112482.
- [153] Q. Luo, X. Huang, Y. Luo, H. Yuan, T. Ren, X. Li, D. Xu, X. Guo, Y. Wu, Fluorescent chitosan-based hydrogel incorporating titanate and cellulose nanofibers modified with carbon dots for adsorption and detection of Cr(VI), *Chem. Eng. J.*, 407 (2021) 127050, doi: 10.1016/j.cej.2020.127050.
- [154] S. Zhang, Y. Dong, Z. Yang, W. Yang, J. Wu, C. Dong, Adsorption of pharmaceuticals on chitosan-based magnetic composite particles with core-brush topology, *Chem. Eng. J.*, 304 (2016) 325–334.
- [155] M. Raeiszadeh, A. Hakimian, A. Shojaei, H. Molavi, Nanodiamond-filled chitosan as an efficient adsorbent for anionic dye removal from aqueous solutions, *J. Environ. Chem. Eng.*, 6 (2018) 3283–3294.
- [156] M.H. Farzana, S. Meenakshi, Decolorization and detoxification of Acid blue 158 dye using cuttlefish bone powder as co-adsorbent via photocatalytic method, *J. Water Process Eng.*, 2 (2014) 22–30.
- [157] M.S. Almughamisi, Z.A. Khan, W. Alshitari, K.Z. Elwakeel, Recovery of chromium(VI) oxyanions from aqueous solution using Cu(OH)<sub>2</sub> and CuO embedded chitosan adsorbents, *J. Polym. Environ.*, 28 (2020) 47–60.
- [158] T.D. Mashangwa, An Investigation Into the Efficacy of Eggshells as a Low-Cost Adsorbent for the Removal of Potentially Toxic Inorganic Elements From Aqueous Solutions, M.Sc. Dissertation, University of South Africa, 2016.
- [159] A. Azari, M. Noorisepehr, E. Dehghanifard, K. Karimyan, S.Y. Hashemi, E.M. Kalhori, R. Norouzi, S. Agarwal, V.K. Gupta, Experimental design, modeling and mechanism of cationic dyes biosorption on to magnetic chitosan-alutaraldehyde composite, *Int. J. Biol. Macromol.*, 131 (2019) 633–645.
- [160] I.A. Lawal, D. Chetty, S.O. Akpotu, B. Moodley, Sorption of Congo red and reactive blue on biomass and activated carbon derived from biomass modified by ionic liquid, *Environ. Nanotechnol. Monit. Manage.*, 8 (2017) 83–91.
- [161] N. Tka, M. Jabli, T.A. Saleh, G.A. Salman, Amines modified fibers obtained from natural *Populus tremula* and their rapid biosorption of Acid blue 25, *J. Mol. Liq.*, 250 (2018) 423–432.
- [162] A.P. de Oliveira, A.N. Módenes, M.E. Bragião, C.L. Hinterholz, D.E.G. Trigueros, I.G. de O. Bezerra, Use of grape pomace as a biosorbent for the removal of the Brown KROM KGT dye, *Bioresour. Technol. Rep.*, 2 (2018) 92–99.
- [163] A.B. Albadarin, S. Solomon, T.A. Kurniawan, C. Mangwandi, G. Walker, Single, simultaneous and consecutive biosorption of Cr(VI) and Orange II onto chemically modified masau stones, *J. Environ. Manage.*, 204 (2017) 365–374.
- [164] Q. Kong, X. Wang, T. Lou, Preparation of millimeter-sized chitosan/carboxymethyl cellulose hollow capsule and its dye adsorption properties, *Carbohydr. Polym.*, 244 (2020) 116481, doi: 10.1016/j.carbpol.2020.116481.
- [165] A.S. Al-Wasidi, I.I.S. AlZahrani, H.I. Thawibaraka, A.M. Naglah, M.G. El-Desouky, M.A. El-Bindary, Adsorption studies of carbon dioxide and anionic dye on green adsorbent, *J. Mol. Struct.*, 1250 (2021) 131736, doi: 10.1016/j.molstruc.2021.131736.
- [166] N. Aarab, A. Hsini, M. Laabd, A. Esseki, T. Laktif, M.A. Haki, R. Lakhmiri, A. Albourine, Theoretical study of the adsorption of sodium salicylate and metronidazole on the PANi, *Mater. Today. Proc.*, 22 (2020) 100–103.
- [167] E. Bazrafshan, S. Ahmadi, Removal COD of landfill leachate using coagulation and activated tea waste (ZnCl<sub>2</sub>) adsorption, *Int. J. Innovation Sci. Eng. Technol.*, 4 (2017) 339–347.
- [168] I. Langmuir, The adsorption of gases on plane surfaces of glass, mica and platinum, *J. Am. Ceram. Soc.*, 40 (1918) 1361–1403.

- [169] H. Freundlich, W. Heller, The adsorption of cis- and trans-azobenzene, *J. Am. Chem. Soc.*, 61 (1939) 2228–2230.
- [170] M.M. Dubinin, E. Zaverina, L. Radushkevich, Sorption and structure of active carbons. I. Adsorption of organic vapors, *J. Zhurnal Fizicheskoi Khimii*, 21 (1947) 151–162.
- [171] M.J. Temkin, V. Pyzhev, Recent modifications to Langmuir isotherms, *Acta Physicochim. URSS*, 12 (1940) 217–225.
- [172] M.G. El-Desouky, A. Shahat, A.A. El-Bindary, M.A. El-Bindary, Description, kinetic and equilibrium studies of the adsorption of carbon dioxide in mesoporous iron oxide nanospheres, *Biointerface Res. Appl. Chem.*, 12 (2021) 1022–1038.
- [173] N. Hassan, A. Shahat, A. El-Didamony, M. El-Desouky, A. El-Bindary, Mesoporous iron oxide nano spheres for capturing organic dyes from water sources, *J. Mol. Struct.*, 1217 (2020) 128361, doi: 10.1016/j.molstruc.2020.128361.
- [174] K. Elwakeel, A. El-Bindary, A. Ismail, A. Morshidy, Sorptive removal of Remazol Brilliant Blue R from aqueous solution by diethylenetriamine functionalized magnetic macro-reticular hybrid material, *RSC Adv.*, 6 (2016) 22395–22410.
- [175] J. Zeldowitsch, Über den mechanismus der katalytischen oxydation von CO an  $MnO_2$ , *Acta Physicochim. URSS*, 1 (1934) 364–449.
- [176] N. Hassan, A. Shahat, A. El-Didamony, M.G. El-Desouky, A.A. El-Bindary, Equilibrium, kinetic and thermodynamic studies of adsorption of cationic dyes from aqueous solution using ZIF-8, *Moroccan J. Chem.*, 8 (2020) 2627–2637.
- [177] H.A. Kiwaan, F.S. Mohamed, N.A. El-Ghamaz, N.M. Beshry, A.A. El-Bindary, Experimental and electrical studies of zeolitic imidazolate framework-8 for the adsorption of different dyes, *J. Mol. Liq.*, 338 (2021) 116670, doi: 10.1016/j.molliq.2021.116670.
- [178] M. Haghighizadeh, K. Zare, H. Aghaie, M. Monajjemi, Preparation and characterization of Chicory leaf powder and its application as a nano-native plant sorbent for removal of Acid blue 25 from aqueous media: isotherm, kinetic and thermodynamic study of the adsorption phenomenon, *J. Nanostruct. Chem.*, 10 (2020) 75–86.
- [179] S. Rahdar, A. Rahdar, M.N. Zafar, S.S. Shafqat, S. Ahmadi, Synthesis and characterization of MgO supported Fe–Co–Mn nanoparticles with exceptionally high adsorption capacity for Rhodamine B dye, *J. Mater. Process. Technol.*, 8 (2019) 3800–3810.
- [180] C.I. Oprea, P. Panait, F. Cimpoesu, M. Ferbinteanu, M.A. Gîrțu, Density functional theory (DFT) study of coumarin-based dyes adsorbed on  $TiO_2$  nanoclusters – applications to dye-sensitized solar cells, *Materials*, 6 (2013) 2372–2392.
- [181] Y. Achour, M. Khouili, H. Abderrafia, S. Melliani, M.R. Laamari, M. El Haddad, DFT investigations and experimental studies for competitive and adsorptive removal of two cationic dyes onto an eco-friendly material from aqueous media, *Int. J. Environ. Res.*, 12 (2018) 789–802.
- [182] X. Liu, R. Wang, Z. Ni, W. Zhou, Y. Du, Z. Ye, R. Guo, Facile synthesis and selective adsorption properties of  $Sm_2CuO_4$  for malachite green: kinetics, thermodynamics and DFT studies, *J. Alloys Compd.*, 743 (2018) 17–25.
- [183] H. Luo, X. Huang, Y. Luo, Z. Li, L. Li, C. Gao, J. Xiong, W. Li, Adsorption behavior and mechanism of acidic blue 25 dye onto cucurbit [8] uril: a spectral and DFT study, *Spectrochim. Acta, Part A*, 193 (2018) 125–132.
- [184] R. El Haouti, H. Ouachtak, A. El Guerdaoui, A. Amedlous, E. Amaterz, R. Haounati, A.A. Addi, F. Akbal, N. El Alem, M.L. Taha, Cationic dyes adsorption by Na-montmorillonite nano clay: experimental study combined with a theoretical investigation using DFT-based descriptors and molecular dynamics simulations, *J. Mol. Liq.*, 290 (2019) 111139, doi: 10.1016/j.molliq.2019.111139.
- [185] A. Nakhli, M. Bergaoui, K.-H. Toumi, M. Khalfaoui, Y. Benguerba, M. Balsamo, F.E. Soetaredjo, S. Ismadji, B. Ernst, A. Erto, Molecular insights through computational modeling of methylene blue adsorption onto low-cost adsorbents derived from natural materials: a multi-model's approach, *Comput. Chem. Eng.*, 140 (2020) 106965, doi: 10.1016/j.compchemeng.2020.106965.
- [186] G.A.A. AlHazmi, Kh.S. AbouMelha, M.G. El-Desouky, A.A. El-Bindary, Effective adsorption of doxorubicin hydrochloride on zirconium metal-organic framework: equilibrium, kinetic and thermodynamic studies, *J. Mol. Struct.*, 1258 (2022) 132679, doi: 10.1016/j.molstruc.2022.132679.
- [187] Y.-H. Lin, H.-T. Jeng, D.-S. Lin, Separation of the attractive and repulsive contributions to the adsorbate–adsorbate interactions of polar adsorbates on Si (100), *Surf. Sci.*, 641 (2015) 282–288.
- [188] A.S. Al-Wasidi, I.I.S. AlZahrani, A.M. Naglah, M.G. El-Desouky, M.A. Khalil, A.A. El-Bindary, M.A. El-Bindary, Effective removal of methylene blue from aqueous solution using metal–organic framework; modelling analysis, statistical physics treatment and DFT calculations, *ChemistrySelect*, 6 (2021) 11431–11447.

## Supporting information

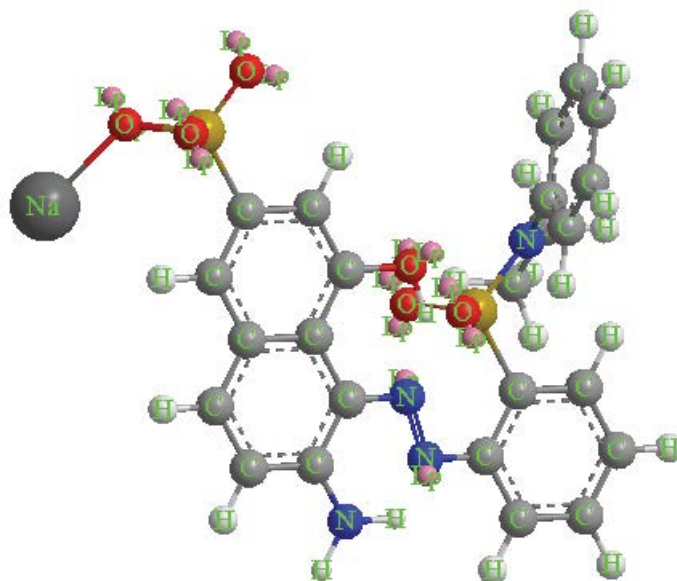


Fig. S1. Acid red 57.

Table S1  
Bond length at Acid red 57

Atom	Actual (Å)	Optimum (Å)	Atom	Actual (Å)	Optimum (Å)
O(35)-Lp(72)	0.600	0.600	C(25)-C(26)	1.395	1.420
O(35)-Lp(71)	0.600	0.600	C(24)-C(25)	1.395	1.420
O(34)-Lp(70)	0.600	0.600	C(23)-C(24)	1.395	1.420
O(34)-Lp(69)	0.600	0.600	C(22)-C(23)	1.395	1.420
O(31)-Lp(68)	0.600	0.600	C(15)-C(20)	1.395	1.420
O(31)-Lp(67)	0.600	0.600	C(19)-C(20)	1.395	1.420
O(30)-Lp(66)	0.600	0.600	C(18)-C(19)	1.395	1.420
O(30)-Lp(65)	0.600	0.600	C(17)-C(18)	1.395	1.420
O(29)-Lp(64)	0.600	0.600	C(16)-C(17)	1.395	1.420
O(29)-Lp(63)	0.600	0.600	C(15)-C(16)	1.395	1.420
N(14)-Lp(62)	0.600	0.600	C(6)-C(5)	1.396	1.420
N(13)-Lp(61)	0.600	0.600	C(4)-C(5)	1.404	1.420
O(11)-Lp(60)	0.600	0.600	C(3)-C(4)	1.414	1.420
O(11)-Lp(59)	0.600	0.600	C(10)-C(4)	1.404	1.420
C(37)-H(58)	1.113	1.113	C(9)-C(10)	1.396	1.420
C(37)-H(57)	1.113	1.113	C(8)-C(9)	1.392	1.420
C(36)-H(56)	1.113	1.113	C(7)-C(8)	1.396	1.420
C(36)-H(55)	1.113	1.113	C(3)-C(7)	1.404	1.420
C(36)-H(54)	1.113	1.113	C(2)-C(3)	1.404	1.420
C(27)-H(53)	1.100	1.100	C(1)-C(2)	1.396	1.420
C(26)-H(52)	1.100	1.100	C(6)-C(1)	1.392	1.420
C(25)-H(51)	1.100	1.100	N(21)-C(22)	1.266	1.462
C(24)-H(50)	1.100	1.100	N(21)-C(37)	1.470	1.470
C(23)-H(49)	1.100	1.100	S(33)-N(21)	1.696	
C(19)-H(48)	1.100	1.100	C(20)-S(33)	1.790	
C(18)-H(47)	1.100	1.100	N(14)-C(15)	1.260	1.456
C(17)-H(46)	1.100	1.100	N(13)-N(14)	1.248	1.248
C(16)-H(45)	1.100	1.100	C(7)-N(13)	1.260	1.456
N(12)-H(44)	1.050	1.050	C(8)-N(12)	1.266	1.462
N(12)-H(43)	1.050	1.050	C(2)-O(11)	1.355	1.355
O(11)-H(42)	0.972	0.972	C(6)-S(28)	1.790	
C(10)-H(41)	1.100	1.100	C(36)-C(37)	1.523	1.523
C(9)-H(40)	1.100	1.100	S(33)-O(35)	1.450	1.450
C(5)-H(39)	1.100	1.100	S(33)-O(34)	1.450	1.450
C(1)-H(38)	1.100	1.100	S(28)-O(31)	1.660	
C(22)-C(27)	1.395	1.420	S(28)-O(30)	1.450	1.450
C(26)-C(27)	1.395	1.420	S(28)-O(29)	1.450	1.450
			O(31)-Na(32)	2.180	

Table S2  
Bond angle of Acid red 57

Atom	Actual (Å)	Optimum (Å)	Atom	Actual (Å)	Optimum (Å)
H(58)-C(37)-H(57)	109.520	109.400	C(26)-C(25)-C(24)	120.003	
H(58)-C(37)-N(21)	109.462		H(50)-C(24)-C(25)	120.000	120.000
H(58)-C(37)-C(36)	109.462	109.410	H(50)-C(24)-C(23)	120.000	120.000
H(57)-C(37)-N(21)	109.442		C(25)-C(24)-C(23)	120.000	
H(57)-C(37)-C(36)	109.442	109.410	H(49)-C(23)-C(24)	120.002	120.000
N(21)-C(37)-C(36)	109.500		H(49)-C(23)-C(22)	120.002	120.000
H(56)-C(36)-H(55)	109.520	109.000	C(24)-C(23)-C(22)	119.997	
H(56)-C(36)-H(54)	109.462	109.000	C(27)-C(22)-C(23)	120.003	120.000
H(56)-C(36)-C(37)	109.462	110.000	C(27)-C(22)-N(21)	119.999	120.000
H(55)-C(36)-H(54)	109.442	109.000	C(23)-C(22)-N(21)	119.999	120.000
H(55)-C(36)-C(37)	109.442	110.000	C(22)-N(21)-C(37)	120.000	108.000
H(54)-C(36)-C(37)	109.500	110.000	C(22)-N(21)-S(33)	120.000	
Lp(72)-O(35)-Lp(71)	120.000	131.000	C(37)-N(21)-S(33)	120.000	
Lp(72)-O(35)-S(33)	120.000		C(15)-C(20)-C(19)	120.000	120.000
Lp(71)-O(35)-S(33)	120.000		C(15)-C(20)-S(33)	120.000	
Lp(70)-O(34)-Lp(69)	120.000	131.000	C(19)-C(20)-S(33)	120.000	
Lp(70)-O(34)-S(33)	120.000		H(48)-C(19)-C(20)	120.001	120.000
Lp(69)-O(34)-S(33)	120.000		H(48)-C(19)-C(18)	120.001	120.000
N(21)-S(33)-C(20)	109.462		C(20)-C(19)-C(18)	119.997	
N(21)-S(33)-O(35)	109.520		H(47)-C(18)-C(19)	119.998	120.000
N(21)-S(33)-O(34)	109.462		H(47)-C(18)-C(17)	119.998	120.000
C(20)-S(33)-O(35)	109.442		C(19)-C(18)-C(17)	120.003	
C(20)-S(33)-O(34)	109.500		H(46)-C(17)-C(18)	120.000	120.000
O(35)-S(33)-O(34)	109.442	116.600	H(46)-C(17)-C(16)	120.000	120.000
Lp(68)-O(31)-Lp(67)	117.390	131.000	C(18)-C(17)-C(16)	120.000	
Lp(68)-O(31)-S(28)	103.298		H(45)-C(16)-C(17)	120.002	120.000
Lp(68)-O(31)-Na(32)	103.298		H(45)-C(16)-C(15)	120.002	120.000
Lp(67)-O(31)-S(28)	106.760		C(17)-C(16)-C(15)	119.997	
Lp(67)-O(31)-Na(32)	106.760		C(20)-C(15)-C(16)	120.003	120.000
S(28)-O(31)-Na(32)	120.000		C(20)-C(15)-N(14)	119.999	120.000
Lp(66)-O(30)-Lp(65)	120.000	131.000	C(16)-C(15)-N(14)	119.999	120.000
Lp(66)-O(30)-S(28)	120.000		Lp(62)-N(14)-C(15)	109.939	122.500
Lp(65)-O(30)-S(28)	120.000		Lp(62)-N(14)-N(13)	109.939	120.000
Lp(64)-O(29)-Lp(63)	120.000	131.000	C(15)-N(14)-N(13)	107.500	107.500
Lp(64)-O(29)-S(28)	120.000		Lp(61)-N(13)-N(14)	109.939	120.000
Lp(63)-O(29)-S(28)	120.000		Lp(61)-N(13)-C(7)	109.939	122.500
C(6)-S(28)-O(31)	109.462		N(14)-N(13)-C(7)	107.500	107.500
C(6)-S(28)-O(30)	109.442		H(44)-N(12)-H(43)	120.000	118.800
C(6)-S(28)-O(29)	109.500		H(44)-N(12)-C(8)	120.000	
O(31)-S(28)-O(30)	109.520		H(43)-N(12)-C(8)	120.000	
O(31)-S(28)-O(29)	109.462		Lp(60)-O(11)-Lp(59)	108.537	
O(30)-S(28)-O(29)	109.442	116.600	Lp(60)-O(11)-H(42)	110.335	101.100
H(53)-C(27)-C(22)	120.000	120.000	Lp(60)-O(11)-C(2)	110.335	
H(53)-C(27)-C(26)	120.000	120.000	Lp(59)-O(11)-H(42)	109.815	101.100
C(22)-C(27)-C(26)	120.000		Lp(59)-O(11)-C(2)	109.815	
H(52)-C(26)-C(27)	120.001	120.000	H(42)-O(11)-C(2)	108.000	108.000
H(52)-C(26)-C(25)	120.001	120.000	H(41)-C(10)-C(4)	119.626	120.000
C(27)-C(26)-C(25)	119.997		H(41)-C(10)-C(9)	119.626	120.000
H(51)-C(25)-C(26)	119.998	120.000	C(4)-C(10)-C(9)	120.747	
H(51)-C(25)-C(24)	119.998	120.000	H(40)-C(9)-C(10)	120.007	120.000
			H(40)-C(9)-C(8)	120.007	120.000
			C(10)-C(9)-C(8)	119.987	

Atom	Actual (Å)	Optimum (Å)	Atom	Actual (Å)	Optimum (Å)
C(9)-C(8)-C(7)	119.994	120.000	C(5)-C(4)-C(3)	119.266	120.000
C(9)-C(8)-N(12)	120.003	120.000	C(5)-C(4)-C(10)	121.470	120.000
C(7)-C(8)-N(12)	120.003	120.000	C(3)-C(4)-C(10)	119.264	120.000
C(8)-C(7)-C(3)	120.738	120.000	C(4)-C(3)-C(7)	119.270	120.000
C(8)-C(7)-N(13)	119.631	120.000	C(4)-C(3)-C(2)	119.266	120.000
C(3)-C(7)-N(13)	119.631	120.000	C(7)-C(3)-C(2)	121.464	120.000
C(5)-C(6)-C(1)	119.986	120.000	C(3)-C(2)-C(1)	120.741	120.000
C(5)-C(6)-S(28)	120.007		C(3)-C(2)-O(11)	119.630	124.300
C(1)-C(6)-S(28)	120.007		C(1)-C(2)-O(11)	119.630	124.300
H(39)-C(5)-C(6)	119.627	120.000	H(38)-C(1)-C(2)	120.002	120.000
H(39)-C(5)-C(4)	119.627	120.000	H(38)-C(1)-C(6)	120.002	120.000
C(6)-C(5)-C(4)	120.746		C(2)-C(1)-C(6)	119.996	

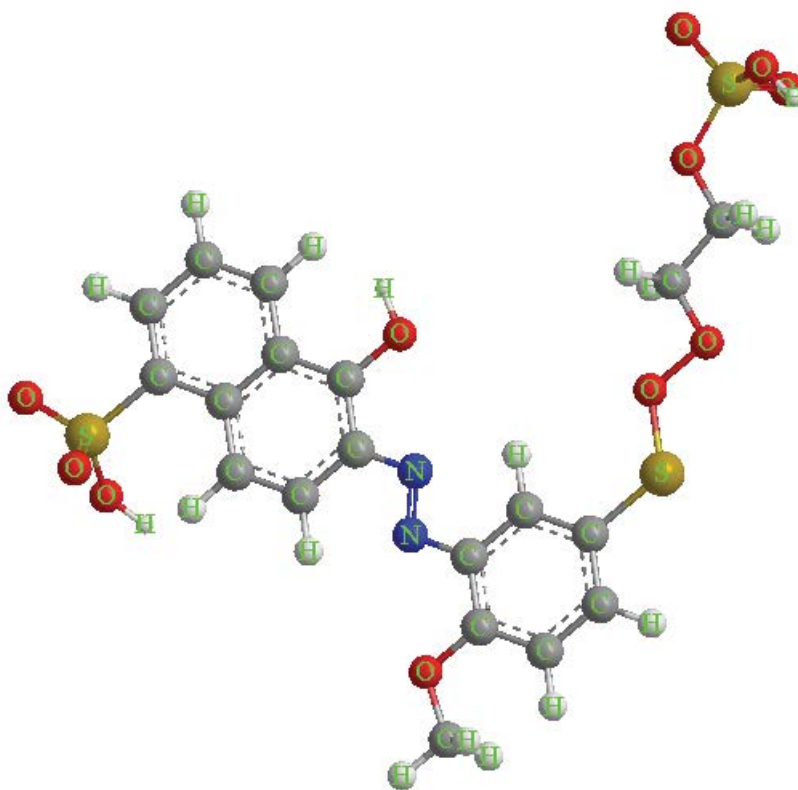


Fig. S2. Remazol red.

Table S3  
Bond length of Remazol red

Atom	Actual (Å)	Optimum (Å)
O(35)-H(53)	0.942	0.942
C(28)-H(52)	1.113	1.111
C(28)-H(51)	1.113	1.111
C(28)-H(50)	1.113	1.111
O(26)-H(49)	0.942	0.942
C(21)-H(48)	1.113	1.111
C(21)-H(47)	1.113	1.111
C(20)-H(46)	1.113	1.111
C(20)-H(45)	1.113	1.111
C(19)-H(44)	1.100	1.100
C(17)-H(43)	1.100	1.100
C(16)-H(42)	1.100	1.100
O(11)-H(41)	0.972	0.972
C(10)-H(40)	1.100	1.100
C(9)-H(39)	1.100	1.100
C(6)-H(38)	1.100	1.100
C(5)-H(37)	1.100	1.100
C(4)-H(36)	1.100	1.100
C(14)-C(19)	1.395	1.420
C(18)-C(19)	1.395	1.420
C(17)-C(18)	1.395	1.420
C(16)-C(17)	1.395	1.420
C(15)-C(16)	1.395	1.420
C(14)-C(15)	1.395	1.420
C(5)-C(6)	1.396	1.420
C(1)-C(6)	1.404	1.420
C(2)-C(1)	1.414	1.420
C(7)-C(1)	1.404	1.420
C(8)-C(7)	1.396	1.420
C(9)-C(8)	1.392	1.420
C(10)-C(9)	1.396	1.420
C(2)-C(10)	1.404	1.420
C(3)-C(2)	1.404	1.420
C(4)-C(3)	1.396	1.420
C(5)-C(4)	1.392	1.420
C(21)-C(20)	1.523	1.505
O(22)-S(32)	1.660	
C(21)-O(22)	1.402	1.389
O(29)-C(20)	1.402	1.398
C(18)-S(31)	1.815	1.815
C(15)-O(27)	1.355	1.355
N(13)-C(14)	1.260	1.456
N(12)-N(13)	1.248	1.248
C(8)-N(12)	1.260	1.456
C(7)-O(11)	1.355	1.355
C(3)-S(23)	1.790	
S(32)-O(35)	1.660	
S(32)-O(34)	1.450	1.450
S(32)-O(33)	1.450	1.450
O(29)-O(30)	1.428	1.437

Atom	Actual (Å)	Optimum (Å)
O(30)-S(31)	1.660	
O(27)-C(28)	1.402	1.396
S(23)-O(26)	1.660	
S(23)-O(25)	1.450	1.450
S(23)-O(24)	1.450	1.450

Table S4  
Bond angle of Remazol red

Atom	Actual (Å)	Optimum (Å)
H(53)-O(35)-S(32)	120.000	
O(22)-S(32)-O(35)	109.462	
O(22)-S(32)-O(34)	109.442	
O(22)-S(32)-O(33)	109.500	
O(35)-S(32)-O(34)	109.520	
O(35)-S(32)-O(33)	109.462	
O(34)-S(32)-O(33)	109.442	116.600
C(18)-S(31)-O(30)	120.000	
O(29)-O(30)-S(31)	120.000	
C(20)-O(29)-O(30)	98.700	98.700
H(52)-C(28)-H(51)	109.520	109.000
H(52)-C(28)-H(50)	109.462	109.000
H(52)-C(28)-O(27)	109.462	106.700
H(51)-C(28)-H(50)	109.442	109.000
H(51)-C(28)-O(27)	109.442	106.700
H(50)-C(28)-O(27)	109.500	106.700
C(15)-O(27)-C(28)	110.800	110.800
H(49)-O(26)-S(23)	120.000	
C(3)-S(23)-O(26)	109.462	
C(3)-S(23)-O(25)	109.442	
C(3)-S(23)-O(24)	109.500	
O(26)-S(23)-O(25)	109.520	
O(26)-S(23)-O(24)	109.462	
O(25)-S(23)-O(24)	109.442	116.600
S(32)-O(22)-C(21)	120.000	
H(48)-C(21)-H(47)	109.520	109.400
H(48)-C(21)-C(20)	109.462	109.410
H(48)-C(21)-O(22)	109.462	106.700
H(47)-C(21)-C(20)	109.442	109.410
H(47)-C(21)-O(22)	109.442	106.700
C(20)-C(21)-O(22)	109.500	107.400
H(46)-C(20)-H(45)	109.520	109.400
H(46)-C(20)-C(21)	109.462	109.410
H(46)-C(20)-O(29)	109.462	106.700
H(45)-C(20)-C(21)	109.442	109.410
H(45)-C(20)-O(29)	109.442	106.700
C(21)-C(20)-O(29)	109.500	107.400
H(44)-C(19)-C(14)	120.000	120.000
H(44)-C(19)-C(18)	120.000	120.000
C(14)-C(19)-C(18)	120.000	
C(19)-C(18)-C(17)	119.997	120.000
C(19)-C(18)-S(31)	120.001	118.000

Atom	Actual (Å)	Optimum (Å)	Atom	Actual (Å)	Optimum (Å)
C(17)-C(18)-S(31)	120.001	118.000	C(7)-C(8)-N(12)	120.007	120.000
H(43)-C(17)-C(18)	119.998	120.000	C(9)-C(8)-N(12)	120.007	120.000
H(43)-C(17)-C(16)	119.998	120.000	C(1)-C(7)-C(8)	120.747	120.000
C(18)-C(17)-C(16)	120.003		C(1)-C(7)-O(11)	119.626	124.300
H(42)-C(16)-C(17)	120.000	120.000	C(8)-C(7)-O(11)	119.626	124.300
H(42)-C(16)-C(15)	120.000	120.000	H(38)-C(6)-C(5)	119.627	120.000
C(17)-C(16)-C(15)	120.000		H(38)-C(6)-C(1)	119.627	120.000
C(16)-C(15)-C(14)	119.997	120.000	C(5)-C(6)-C(1)	120.746	
C(16)-C(15)-O(27)	120.002	124.300	H(37)-C(5)-C(6)	120.007	120.000
C(14)-C(15)-O(27)	120.002	124.300	H(37)-C(5)-C(4)	120.007	120.000
C(19)-C(14)-C(15)	120.003	120.000	C(6)-C(5)-C(4)	119.986	
C(19)-C(14)-N(13)	119.999	120.000	H(36)-C(4)-C(3)	120.002	120.000
C(15)-C(14)-N(13)	119.999	120.000	H(36)-C(4)-C(5)	120.002	120.000
C(14)-N(13)-N(12)	107.500	107.500	C(3)-C(4)-C(5)	119.996	
N(13)-N(12)-C(8)	107.500	107.500	C(2)-C(3)-C(4)	120.741	120.000
H(41)-O(11)-C(7)	108.000	108.000	C(2)-C(3)-S(23)	119.630	
H(40)-C(10)-C(9)	119.631	120.000	C(4)-C(3)-S(23)	119.630	
H(40)-C(10)-C(2)	119.631	120.000	C(1)-C(2)-C(10)	119.270	120.000
C(9)-C(10)-C(2)	120.738		C(1)-C(2)-C(3)	119.266	120.000
H(39)-C(9)-C(8)	120.003	120.000	C(10)-C(2)-C(3)	121.464	120.000
H(39)-C(9)-C(10)	120.003	120.000	C(6)-C(1)-C(2)	119.266	120.000
C(8)-C(9)-C(10)	119.994		C(6)-C(1)-C(7)	121.470	120.000
C(7)-C(8)-C(9)	119.987	120.000	C(2)-C(1)-C(7)	119.264	120.000

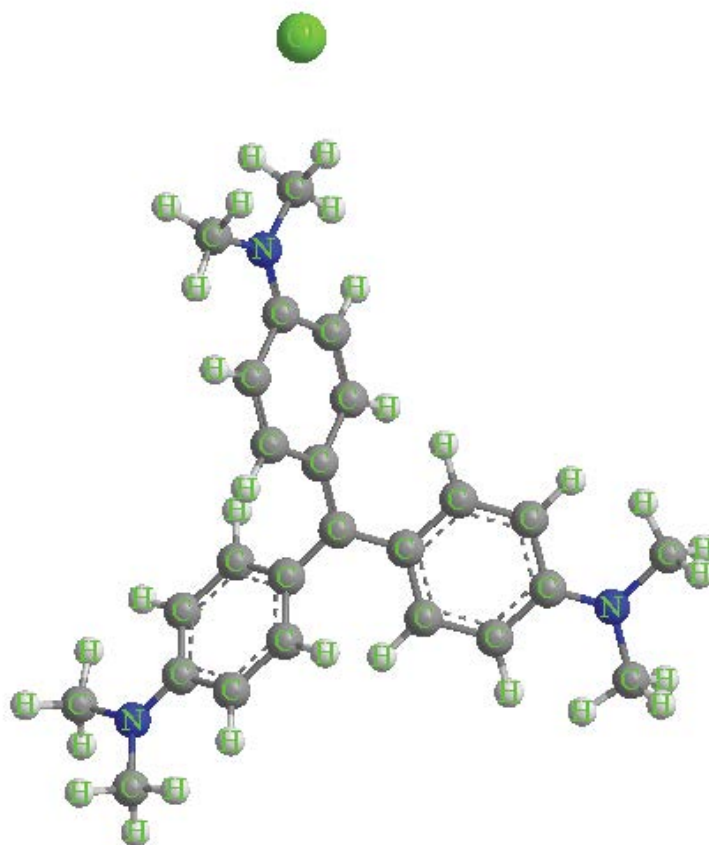


Fig. S3. Crystal violet.

Table S5  
Bond length of crystal violet

Atom	Actual (Å)	Optimum (Å)
C(28)-H(59)	1.113	1.113
C(28)-H(58)	1.113	1.113
C(28)-H(57)	1.113	1.113
C(27)-H(56)	1.113	1.113
C(27)-H(55)	1.113	1.113
C(27)-H(54)	1.113	1.113
C(25)-H(53)	1.100	1.100
C(24)-H(52)	1.100	1.100
C(22)-H(51)	1.100	1.100
C(21)-H(50)	1.100	1.100
C(20)-H(49)	1.113	1.113
C(20)-H(48)	1.113	1.113
C(20)-H(47)	1.113	1.113
C(19)-H(46)	1.113	1.113
C(19)-H(45)	1.113	1.113
C(19)-H(44)	1.113	1.113
C(17)-H(43)	1.100	1.100
C(16)-H(42)	1.100	1.100
C(14)-H(41)	1.100	1.100
C(13)-H(40)	1.100	1.100
C(9)-H(39)	1.113	1.113
C(9)-H(38)	1.113	1.113
C(9)-H(37)	1.113	1.113
C(8)-H(36)	1.113	1.113
C(8)-H(35)	1.113	1.113
C(8)-H(34)	1.113	1.113
C(5)-H(33)	1.100	1.100
C(4)-H(32)	1.100	1.100
C(2)-H(31)	1.100	1.100
C(1)-H(30)	1.100	1.100
C(11)-C(25)	1.395	1.420
C(24)-C(25)	1.395	1.420
C(23)-C(24)	1.395	1.420
C(22)-C(23)	1.395	1.420
C(21)-C(22)	1.395	1.420
C(11)-C(21)	1.395	1.420
C(13)-C(12)	1.504	1.503
C(17)-C(12)	1.504	1.503
C(16)-C(17)	1.343	1.337
C(15)-C(16)	1.504	1.503
C(14)-C(15)	1.504	1.503
C(13)-C(14)	1.343	1.337
C(1)-C(6)	1.395	1.420
C(5)-C(6)	1.395	1.420
C(4)-C(5)	1.395	1.420
C(3)-C(4)	1.395	1.420
C(2)-C(3)	1.395	1.420
C(1)-C(2)	1.395	1.420
N(26)-C(28)	1.470	1.470
N(26)-C(27)	1.470	1.470

Atom	Actual (Å)	Optimum (Å)
C(23)-N(26)	1.266	1.462
N(18)-C(20)	1.500	1.500
N(18)-C(19)	1.500	1.500
C(15)-N(18)	1.300	1.300
C(10)-C(12)	1.337	1.337
C(10)-C(11)	1.337	1.503
C(3)-C(10)	1.337	1.503
N(7)-C(9)	1.470	1.470
N(7)-C(8)	1.470	1.470
C(6)-N(7)	1.266	1.462

Table S6  
Bond angle of crystal violet

Atom	Actual (Å)	Optimum (Å)
H(59)-C(28)-H(58)	109.520	109.000
H(59)-C(28)-H(57)	109.462	109.000
H(59)-C(28)-N(26)	109.462	
H(58)-C(28)-H(57)	109.442	109.000
H(58)-C(28)-N(26)	109.442	
H(57)-C(28)-N(26)	109.500	
H(56)-C(27)-H(55)	109.520	109.000
H(56)-C(27)-H(54)	109.462	109.000
H(56)-C(27)-N(26)	109.462	
H(55)-C(27)-H(54)	109.442	109.000
H(55)-C(27)-N(26)	109.442	
H(54)-C(27)-N(26)	109.500	
C(28)-N(26)-C(27)	120.000	
C(28)-N(26)-C(23)	120.000	108.000
C(27)-N(26)-C(23)	120.000	108.000
H(53)-C(25)-C(11)	120.000	120.000
H(53)-C(25)-C(24)	120.000	120.000
C(11)-C(25)-C(24)	120.000	
H(52)-C(24)-C(25)	120.001	120.000
H(52)-C(24)-C(23)	120.001	120.000
C(25)-C(24)-C(23)	119.997	
C(24)-C(23)-C(22)	120.003	120.000
C(24)-C(23)-N(26)	119.998	120.000
C(22)-C(23)-N(26)	119.998	120.000
H(51)-C(22)-C(23)	120.000	120.000
H(51)-C(22)-C(21)	120.000	120.000
C(23)-C(22)-C(21)	120.000	
H(50)-C(21)-C(22)	120.002	120.000
H(50)-C(21)-C(11)	120.002	120.000
C(22)-C(21)-C(11)	119.997	
H(49)-C(20)-H(48)	109.520	109.000
H(49)-C(20)-H(47)	109.462	109.000
H(49)-C(20)-N(18)	109.462	
H(48)-C(20)-H(47)	109.442	109.000
H(48)-C(20)-N(18)	109.442	
H(47)-C(20)-N(18)	109.500	
H(46)-C(19)-H(45)	109.520	109.000

Atom	Actual (Å)	Optimum (Å)	Atom	Actual (Å)	Optimum (Å)
H(46)-C(19)-H(44)	109.462	109.000	H(39)-C(9)-H(37)	109.462	109.000
H(46)-C(19)-N(18)	109.462		H(39)-C(9)-N(7)	109.462	
H(45)-C(19)-H(44)	109.442	109.000	H(38)-C(9)-H(37)	109.442	109.000
H(45)-C(19)-N(18)	109.442		H(38)-C(9)-N(7)	109.442	
H(44)-C(19)-N(18)	109.500		H(37)-C(9)-N(7)	109.500	
C(20)-N(18)-C(19)	120.000	117.200	H(36)-C(8)-H(35)	109.520	109.000
C(20)-N(18)-C(15)	120.000	121.400	H(36)-C(8)-H(34)	109.462	109.000
C(19)-N(18)-C(15)	120.000	121.400	H(36)-C(8)-N(7)	109.462	
H(43)-C(17)-C(12)	118.376	120.000	H(35)-C(8)-H(34)	109.442	109.000
H(43)-C(17)-C(16)	118.376	120.000	H(35)-C(8)-N(7)	109.442	
C(12)-C(17)-C(16)	123.248		H(34)-C(8)-N(7)	109.500	
H(42)-C(16)-C(17)	118.380	120.000	C(9)-N(7)-C(8)	120.000	
H(42)-C(16)-C(15)	118.380	120.000	C(9)-N(7)-C(6)	120.000	108.000
C(17)-C(16)-C(15)	123.240		C(8)-N(7)-C(6)	120.000	108.000
C(16)-C(15)-C(14)	113.511	120.000	C(1)-C(6)-C(5)	120.000	120.000
C(16)-C(15)-N(18)	123.244	120.000	C(1)-C(6)-N(7)	120.000	120.000
C(14)-C(15)-N(18)	123.244	120.000	C(5)-C(6)-N(7)	120.000	120.000
H(41)-C(14)-C(15)	118.377	120.000	H(33)-C(5)-C(6)	120.001	120.000
H(41)-C(14)-C(13)	118.377	120.000	H(33)-C(5)-C(4)	120.001	120.000
C(15)-C(14)-C(13)	123.245		C(6)-C(5)-C(4)	119.997	
H(40)-C(13)-C(12)	118.377	120.000	H(32)-C(4)-C(5)	119.998	120.000
H(40)-C(13)-C(14)	118.377	120.000	H(32)-C(4)-C(3)	119.998	120.000
C(12)-C(13)-C(14)	123.246		C(5)-C(4)-C(3)	120.003	
C(13)-C(12)-C(17)	113.508	120.000	C(4)-C(3)-C(2)	120.000	120.000
C(13)-C(12)-C(10)	123.246	120.000	C(4)-C(3)-C(10)	120.000	120.000
C(17)-C(12)-C(10)	123.246	120.000	C(2)-C(3)-C(10)	120.000	120.000
C(25)-C(11)-C(21)	120.003	120.000	H(31)-C(2)-C(3)	120.002	120.000
C(25)-C(11)-C(10)	120.000	120.000	H(31)-C(2)-C(1)	120.002	120.000
C(21)-C(11)-C(10)	119.997	120.000	C(3)-C(2)-C(1)	119.997	
C(12)-C(10)-C(11)	120.000	120.000	H(30)-C(1)-C(6)	119.999	120.000
C(12)-C(10)-C(3)	120.000	120.000	H(30)-C(1)-C(2)	119.999	120.000
C(11)-C(10)-C(3)	120.000	120.000	C(6)-C(1)-C(2)	120.003	
H(39)-C(9)-H(38)	109.520	109.000			

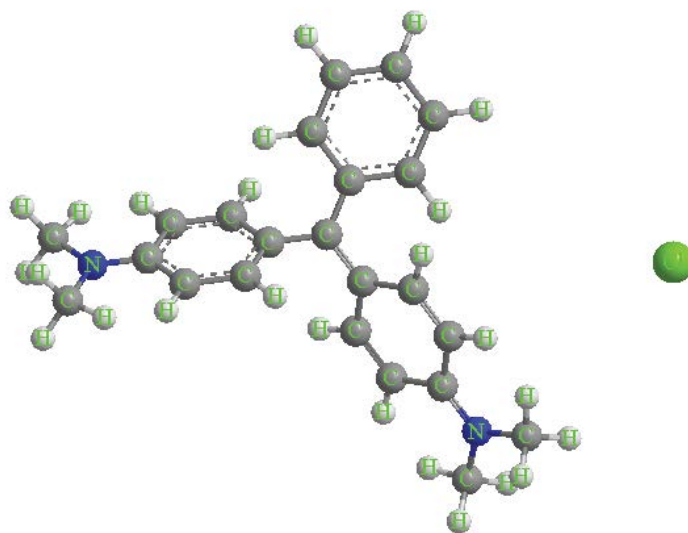


Fig. S4. Malachite green.

Table S7  
Bond length of crystal violet

Atom	Actual (Å)	Optimum (Å)
C(25)-H(51)	1.113	1.113
C(25)-H(50)	1.113	1.113
C(25)-H(49)	1.113	1.113
C(24)-H(48)	1.113	1.113
C(24)-H(47)	1.113	1.113
C(24)-H(46)	1.113	1.113
C(23)-H(45)	1.113	1.113
C(23)-H(44)	1.113	1.113
C(23)-H(43)	1.113	1.113
C(21)-H(42)	1.113	1.113
C(21)-H(41)	1.113	1.113
C(21)-H(40)	1.113	1.113
C(19)-H(39)	1.100	1.100
C(18)-H(38)	1.100	1.100
C(16)-H(37)	1.100	1.100
C(15)-H(36)	1.100	1.100
C(14)-H(35)	1.100	1.100
C(13)-H(34)	1.100	1.100
C(11)-H(33)	1.100	1.100
C(10)-H(32)	1.100	1.100
C(5)-H(31)	1.100	1.100
C(4)-H(30)	1.100	1.100
C(3)-H(29)	1.100	1.100
C(2)-H(28)	1.100	1.100
C(1)-H(27)	1.100	1.100
C(15)-C(8)	1.504	1.503
C(19)-C(8)	1.504	1.503
C(18)-C(19)	1.343	1.337
C(17)-C(18)	1.504	1.503
C(16)-C(17)	1.504	1.503
C(15)-C(16)	1.343	1.337
C(9)-C(14)	1.395	1.420
C(13)-C(14)	1.395	1.420
C(12)-C(13)	1.395	1.420
C(11)-C(12)	1.395	1.420
C(10)-C(11)	1.395	1.420
C(9)-C(10)	1.395	1.420
C(1)-C(6)	1.395	1.420
C(5)-C(6)	1.395	1.420
C(4)-C(5)	1.395	1.420
C(3)-C(4)	1.395	1.420
C(2)-C(3)	1.395	1.420
C(1)-C(2)	1.395	1.420
N(20)-C(25)	1.500	1.500
N(22)-C(24)	1.470	1.470
N(22)-C(23)	1.470	1.470
C(12)-N(22)	1.266	1.462
N(20)-C(21)	1.500	1.500
C(17)-N(20)	1.300	1.300
C(7)-C(9)	1.337	1.503
C(7)-C(8)	1.337	1.337
C(6)-C(7)	1.337	1.503

Table S8  
Bond angle of crystal violet

Atom	Actual (Å)	Optimum (Å)
H(51)-C(25)-H(50)	109.520	109.000
H(51)-C(25)-H(49)	109.462	109.000
H(51)-C(25)-N(20)	109.462	
H(50)-C(25)-H(49)	109.442	109.000
H(50)-C(25)-N(20)	109.442	
H(49)-C(25)-N(20)	109.500	
H(48)-C(24)-H(47)	109.520	109.000
H(48)-C(24)-H(46)	109.462	109.000
H(48)-C(24)-N(22)	109.462	
H(47)-C(24)-H(46)	109.442	109.000
H(47)-C(24)-N(22)	109.442	
H(46)-C(24)-N(22)	109.500	
H(45)-C(23)-H(44)	109.520	109.000
H(45)-C(23)-H(43)	109.462	109.000
H(45)-C(23)-N(22)	109.462	
H(44)-C(23)-H(43)	109.442	109.000
H(44)-C(23)-N(22)	109.442	
H(43)-C(23)-N(22)	109.500	
C(24)-N(22)-C(23)	120.000	
C(24)-N(22)-C(12)	120.000	108.000
C(23)-N(22)-C(12)	120.000	108.000
H(42)-C(21)-H(41)	109.520	109.000
H(42)-C(21)-H(40)	109.462	109.000
H(42)-C(21)-N(20)	109.462	
H(41)-C(21)-H(40)	109.442	109.000
H(41)-C(21)-N(20)	109.442	
H(40)-C(21)-N(20)	109.500	
C(25)-N(20)-C(21)	120.000	117.200
C(25)-N(20)-C(17)	120.000	121.400
C(21)-N(20)-C(17)	120.000	121.400
H(39)-C(19)-C(8)	118.376	120.000
H(39)-C(19)-C(18)	118.376	120.000
C(8)-C(19)-C(18)	123.248	
H(38)-C(18)-C(19)	118.380	120.000
H(38)-C(18)-C(17)	118.380	120.000
C(19)-C(18)-C(17)	123.240	
C(18)-C(17)-C(16)	113.511	120.000
C(18)-C(17)-N(20)	123.244	120.000
C(16)-C(17)-N(20)	123.244	120.000
H(37)-C(16)-C(17)	118.377	120.000
H(37)-C(16)-C(15)	118.377	120.000
C(17)-C(16)-C(15)	123.245	
H(36)-C(15)-C(8)	118.377	120.000
H(36)-C(15)-C(16)	118.377	120.000
C(8)-C(15)-C(16)	123.246	
H(35)-C(14)-C(9)	120.000	120.000
H(35)-C(14)-C(13)	120.000	120.000
C(9)-C(14)-C(13)	120.000	
H(34)-C(13)-C(14)	120.001	120.000
H(34)-C(13)-C(12)	120.001	120.000

Atom	Actual (Å)	Optimum (Å)
C(14)-C(13)-C(12)	119.997	
C(13)-C(12)-C(11)	120.003	120.000
C(13)-C(12)-N(22)	119.998	120.000
C(11)-C(12)-N(22)	119.998	120.000
H(33)-C(11)-C(12)	120.000	120.000
H(33)-C(11)-C(10)	120.000	120.000
C(12)-C(11)-C(10)	120.000	
H(32)-C(10)-C(11)	120.002	120.000
H(32)-C(10)-C(9)	120.002	120.000
C(11)-C(10)-C(9)	119.997	
C(14)-C(9)-C(10)	120.003	120.000
C(14)-C(9)-C(7)	119.999	120.000
C(10)-C(9)-C(7)	119.999	120.000
C(15)-C(8)-C(19)	113.508	120.000
C(15)-C(8)-C(7)	123.246	120.000
C(19)-C(8)-C(7)	123.246	120.000
C(9)-C(7)-C(8)	120.000	120.000
C(9)-C(7)-C(6)	120.000	120.000
C(8)-C(7)-C(6)	120.000	120.000
C(1)-C(6)-C(5)	120.000	120.000
C(1)-C(6)-C(7)	120.000	120.000
C(5)-C(6)-C(7)	120.000	120.000
H(31)-C(5)-C(6)	120.001	120.000
H(31)-C(5)-C(4)	120.001	120.000
C(6)-C(5)-C(4)	119.997	
H(30)-C(4)-C(5)	119.998	120.000
H(30)-C(4)-C(3)	119.998	120.000
C(5)-C(4)-C(3)	120.003	
H(29)-C(3)-C(4)	120.000	120.000
H(29)-C(3)-C(2)	120.000	120.000
C(4)-C(3)-C(2)	120.000	
H(28)-C(2)-C(3)	120.002	120.000
H(28)-C(2)-C(1)	120.002	120.000
C(3)-C(2)-C(1)	119.997	
H(27)-C(1)-C(6)	119.999	120.000
H(27)-C(1)-C(2)	119.999	120.000
C(6)-C(1)-C(2)	120.003	